Cement and Concrete Composites 145 (2024) 105315

Contents lists available at ScienceDirect

Cement and Concrete Composites

journal homepage: www.elsevier.com/locate/cemconcomp

Multi-performance experimental assessment of autogenous and crystalline admixture-stimulated self-healing in UHPFRCCs: Validation and reliability analysis through an inter-laboratory study

Francesco Lo Monte [a,*], Lamija Repesa [a], Didier Snoeck [b,c], Hesam Doostkami [d], Marta Roig-Flores [d,i], Sam J.P. Jackson [e], Ana Blanco Alvarez [e], Milena Nasner [f], Ruben Paul Borg [f], Christof Schröfl [g], Mercedes Giménez [h], Maria Cruz Alonso [h], Pedro Serna [d], Nele De Belie [c], Liberato Ferrara [a]

[a] Department of Civil and Environmental Engineering, Politecnico di Milano, Italy
[b] BATir, École Polytechnique de Bruxelles, Université Libre de Bruxelles, Belgium
[c] Department of Structural Engineering and Building Materials, Ghent University, Belgium
[d] Concrete Science and Technology Institute (ICITECH), Universitat Politecnica de Valencia, Spain
[e] School of Architecture, Building and Civil Engineering, Loughborough University, UK
[f] Faculty for the Built Environment, University of Malta, Malta
[g] Institute of Construction Materials, Technische Universitaet Dresden, Germany
[h] Institute of Construction Science Eduardo Torroja, IETcc-CSIC, Spain
[i] Dep. of Mechanical Engineering and Construction, Universitat Jaume I, Spain

ARTICLE INFO

Keywords:
Self-healing
Crystalline admixtures
Durability
UHPFRCC
Inter-laboratory study

ABSTRACT

The huge benefits brought by the use of Ultra High-Performance Fibre-Reinforced Cementitious Composites (UHPFRCCs) include their high "intrinsic" durability, which is guaranteed by (1) the compact microstructure and (2) the positive interaction between stable multiple-cracking response and autogenous self-healing capability. Hence, self-healing capability must be properly characterized addressing different performances, thus providing all the tools for completely exploiting such large potential. Within this context, the need is clear for a well-established protocol for self-healing characterization. To this end, in the framework of the Cost Action CA15202 SARCOS, six Round Robin Tests involving 30 partners all around Europe were launched addressing different materials, spanning from ordinary concrete to UHPFRCC, and employing different self-healing technologies. In this paper, the tailored experimental methodology is presented and discussed for the specific case of autogenous and crystalline-admixture stimulated healing of UHPFRCC, starting from the comparison of the results from seven different laboratories. The methodology is based on chloride penetration and water permeability tests in cracked disks together with flexural tests on small beams. The latter ones are specifically aimed at assessing the flexural performance recovery of UHPFRCCs, which stands as their signature design "parameter" according to the most recent internationally recognized design approaches. This multi-fold test approach allows to address both inherent durability properties, such as through-crack chloride penetration and apparent water permeability, and more structural/mechanical aspects, such as flexural strength and stiffness.

1. Introduction

The study of concrete self-healing processes and technologies has come to a significant scientific maturity thanks to a relevant number of national and international projects devoted to the topic [1–9] and several large scale and in-situ real applications [10–20].

The state of the art has highlighted that self-healing can represent a powerful resource in the concrete construction industry to rely on more durable and longer lasting structures [21–25], thus also increasing the sustainability of the construction value chain [26–31]. However, even though a great potential hides behind the full exploitation of self-healing, a standard performance assessment framework has not

* Corresponding author.
E-mail address: francesco.lo@polimi.it (F. Lo Monte).

https://doi.org/10.1016/j.cemconcomp.2023.105315
Received 12 June 2023; Received in revised form 29 September 2023; Accepted 4 October 2023
Available online 5 October 2023
0958-9465/© 2023 The Authors. Published by Elsevier Ltd. This is an open access article under the CC BY-NC-ND license (http://creativecommons.org/licenses/by-nc-nd/4.0/).

been defined yet. In particular, standardized test methodologies are needed to quantitatively assess the efficiency of a particular technology with reference to the special performance requirements [32,33].

This highlights the demand for the formulation and validation of a comprehensive approach allowing to quantify the benefits of self-healing, in terms of recovery in both durability and mechanical performances, within a practitioner-friendly framework. Such assessment should be based on reliably and robustly measureable parameters, which require standardized approaches for being monitored and which can be incorporated into durability-based design approaches [34,35]. Furthermore, not only the un-cracked condition has to be entailed, but also the cracked state of the material [10,36], since it represents the most common condition in real structural service scenarios.

Such structured approach could pave the way to a new role for self-healing as a clear-defined capability and no more as a mere bonus in civil structure and infrastructure engineering applications, thus translating into a technological and economical resource [37]. In this regard, the first effort should address the definition of key performance parameters on the base of which healing-induced property-recovery has to be sought, achieved and measured. This view comes from the main principle that self-healing cannot be comprehensively described by one parameter only (and thus assessed by a single experimental test), since concrete performance entails a set of properties which have a different role depending on the specific structural application.

Looking at the literature on the topic, healing is usually assessed (1) through visual evidence of crack closure (this being appropriately referred to as *crack self-sealing* or *surface-crack healing*) or (2) through the recovery of durability-related parameters (such as water capillary absorption, water permeability and chloride diffusion) [38–49]. All the mentioned parameters directly refer to durability, since reduced values result in slower penetration of aggressive agents into concrete and in a slower structural degradation.

Among the influencing aspects in the definition of the assessment framework for self-healing capability, it can be mentioned (1) the type of cementitious material under investigation, (2) the related self-healing technology and (3) the intended final scenario. In a first step, this means distinguishing between Normal-Strength Concrete (NSC) and Ultra High-Performance Fibre-Reinforced Cementitious Composite (UHPFRCC). In the former case, the tension (cracked) region is meant only to provide protection to the reinforcement and concrete itself against the penetration of aggressive agents, while in the latter, the tension (micro-cracked) region sizably contributes to the overall mechanical response.

UHPFRCC, in fact, is characterized by far lower values of durability-related parameters thanks to its compact microstructure and by the ability to spread an otherwise localized crack into a series of thin and tightly spaced multiple cracks. This latter condition is largely positive for UHPFRCC, thanks to the inborn self-healing conduciveness of a narrow crack. In addition, self-healing processes are enhanced by the peculiar mixture composition characterized by high cement and binder contents and low water/binder ratios [50–52], which both provide significant amounts of anhydrous particles for delayed hydration.

The stable multiple cracking response in bending (deflection-hardening behaviour) and/or in tension (strain-hardening behaviour) relies on the bridge-effect provided by structural fibres (metallic, polymeric or organic ones [53]). The role of fibres can be defined through a micro-mechanical approach balancing crack tip toughness and fibre pull-out energy, with benefits for durability (as highlighted before) and increased load bearing capacity [54,55].

In order to properly tackle the twofold advantage brought in by UHPFRCC, the assessment of the healing-induced recovery of the material should address durability/transport properties as well as the mechanical performance, which depends on crack closure and healing-induced improvement in the fibre-matrix interface [56]. Both durability and mechanical response guarantee the stability over time of the structural response in the intended scenario. This makes evident that self-healing assessment should be based on a multiplicity of tests [57].

In order to discuss, in terms of repeatability and consistency, a multi-parameter methodology for self-healing assessment in UHPFRCC [48], a Round Robin Test (RRT) has been launched involving seven different laboratories. It is worth noting that this is one out of six Round Robin Tests launched in the same period focusing on 6 different materials and/or self-healing technologies [48,58–62] (as summarized in Table 1), organized under the umbrella of the COST Action CA15202 SARCOS [5] (Self-healing As prevention Repair of COncrete Structures).

The Round Robin Test on UHPFRCC (RRT4 in Table 1) has involved Politecnico di Milano – PoliMi (Italy), Ghent University – UGent (Belgium), Universitat Politecnica de Valencia – UPV (Spain), Loughborough University – LU (UK), University of Malta – UoM (Malta), Technische Universitaet Dresden – TUD (Germany), and Institute of Construction Science Eduardo Torroja – CSIC (Spain).

The cementitious materials investigated in RRT4 were developed within the Horizon 2020 ReSHEALience project (Rethinking coastal defence and Green-energy Service infrastructures through enHancEd-durAbiLity high-performance cement-based materials) [8,35,49,54,55,57] and were employed for the construction of one of the project full-scale demonstrators, namely a tank containing geothermal water and serving cooling towers in a geothermal power plant.

The data set collected via this inter-laboratory test will also form the basis for further analyses within the framework of the MSCA-ITN SMARTINCS (Self-Healing, Multifunction, Advanced Repair Technologies in Cementitious Systems).

In the multi-test experimental procedure described in the next sections, self-healing is tackled from the points of view of both durability (in terms of transport properties) and mechanical performance. This has been pursued via three different test setups: chloride penetration assessment on cracked disks, water permeability on cracked disks and repeated bending tests on small beams.

The approach allowed investigating different key parameters through "recovery indexes" expected to embrace the main features connected to self-healing, namely durability (intended in a performance-based design framework) and mechanical response. In particular, crack self-sealing capability has been monitored in all the three test types, while recovery in terms of resistance against chloride penetration and water permeability has been studied via tests on disks, and mechanical recovery has been surveyed through repeated bending tests on small beams.

Table 1
Round Robin Tests - RRTs campaign organized within the COST Action CA15202 SARCOS.

	Object		RRT Leader
RRT1	Concrete with mineral additions	[58]	Aristotele University of Technology
RRT2	Concrete with micro-encapsulated additions	[59]	University of Cambridge
RRT3	Concrete with crystalline admixture	[60]	Universitat Politecnica de Valencia
RRT4	UHPFRCC with crystalline admixture	[48]	Politecnico di Milano
RRT5	Concrete with macrocapsules filled with polyurethane	[61]	Ghent University
RRT6	Concrete with encapsulated bacteria	[62]	Technical University of Delft

Table 2
Mix design of UHPFRCC mixtures. (% v_f = volume fraction percentage).

Constituents in [kg/m^3]/[% v_f]	Without (w/o) CA	With (w) CA
Cement CEM I 52.5R	600/19	600/19
Slag	500/19	500/19
Water	200/20	200/20
Steel fibers Azichem Readymix 200®	120/1.5	120/1.5
Sand (0–2 mm)	982/38	982/38
Superplasticizer BASF Glenium ACE 300®	33/3.5	33/3.5
Crystalline admixtures (CA) Penetron Admix®	0.0/0.0	4.8/0.2

2. Materials and experimental plan

2.1. UHPFRCCs' mixture design

The methodology for self-healing assessment has been evaluated by investigating two Ultra-High Performance Fibre-Reinforced Cementitious Composite (UHPFRCC) mixtures (see Table 2), differing only in the presence of crystalline admixture (Penetron Admix®) as self-healing stimulator (the benefits of which have been investigated in Refs. [63–67]).

The volume fraction is about 19 % for cement (c) and slag (s), 38 % for sand (a), 20 % for water (w) (thus resulting into a ratio c:s:a:w close to 1:1:2:1) and 1.5 % for steel fibres. Fibres are characterized by a length of 20 mm and a diameter of 0.22 mm; their amount has been studied in order to obtain a nearly strain-hardening response in tension [54,68].

The composition of the two mixtures is detailed in Table 2. The mixing protocol consisted in mixing all the dry constituents for about 2 min, afterwards adding water and then the superplasticizer. Finally, steel fibres were added, followed by further 10 min of high-speed mixing. The obtained self-levelling consistency guaranteed a proper dispersion of the fibres.

2.2. Testing procedures for self-healing assessment

Following the needs for a multi-performance assessment of self-healing, according to the principles described in the introduction, three tests have been proposed to encompass the main specific features to be recovered by the materials:

1) evaluation of self-healing through the evolution of chloride penetration in pre-cracked disks;
2) evaluation of self-healing through recovery of water permeability in pre-cracked disks;
3) evaluation of self-healing through recovery of mechanical response in four-point bending tests.

All tests are detailed in the next sections together with the description of specimen production, curing conditions and pre-conditioning.

2.2.1. Evolution of chloride penetration on disks

In each laboratory involved in the inter-laboratory study, chloride penetration has been assessed for each mixture on nine concrete disks Ø100 × 80 mm, obtained by cutting three cylinders with dimensions Ø100 × 280 mm.

For each of the two UHPFRCC mixtures, chloride diffusion has been evaluated after 1, 3 and 6 months of continuous immersion in water with 33 g/L of NaCl (thus to simulate a seawater environment), changing the curing bath every month.

At time 0, before immersing the samples in the chloride aqueous solution, six out of the nine concrete disks were *pre-cracked* by splitting up to the target residual crack opening of (100 ± 50) μm, measured after unloading. Such value of crack opening has been chosen since it represents an upper bound of the crack width which can be expected for UHPFRCC (even at high tensile strain regime), as demonstrated by the results regarding the tests on small beams reported in the following sections.

The test setup adopted by PoliMi is reported in Fig. 1, where crack opening has been monitored during splitting by means of three transducers. Very similar test setups have been adopted by the other labs, without any substantial difference. Just after pre-cracking, the lateral face and one of the two circular bases were made waterproof via the application of silicon and tape (blue lines in the scheme of Fig. 2), thus to instate a mostly 1D water flux within the immersed disks.

Image analysis of cracks was performed just after *pre-cracking* at time 0 and at the 3 target healing periods (namely 1, 3 and 6 months after time 0) capturing three microscope images for each diametrical crack of the specimen. Then the average surface crack width has been calculated.

Finally, the *Index of Crack Sealing (ICS)* has been computed as described in Equation (1):

$$ICS\,[-] = 1 - \frac{w_i}{w_{i-1}} \tag{1}$$

In equation (1), w_i is the average crack width at the end of the healing period and w_{i-1} is the average crack width at the beginning of the healing period. In particular, w_{i-1} is the average crack width just after *pre-cracking* for chloride penetration and water permeability tests (since no re-cracking is performed), while it is the average crack width just after previous *re-cracking* for bending tests on thin beams (since re-cracking was performed at each healing duration).

At time 0 all the nine samples (6 pre-cracked and 3 un-cracked) were immersed in salt water. Afterwards, at each target period and for each mixture, chloride penetration was evaluated on two pre-cracked samples and on one un-cracked sample, according to at least one of the two following alternatives: (1) $AgNO_3$ sprayed on the mid split surface (similar to Refs. [32,44,47,48]) or (2) chemical titration (similar to Refs. [32,40,42,46–48]). For both methodologies, no further pre-conditioning has been implemented. A very similar procedure has been extensively used in Ref. [47].

The first approach required the splitting of the disks in two halves with a fracture plane (dashed green lines in Fig. 2) orthogonal to the previous (initial) crack triggered at time 0. In this way, the surface to be

Fig. 1. Pre-cracking of disks as implemented at PoliMi for chloride penetration and permeability tests: (a) front and rear views of the setup, (b) picture of a test and (c) qualitative loading curve.

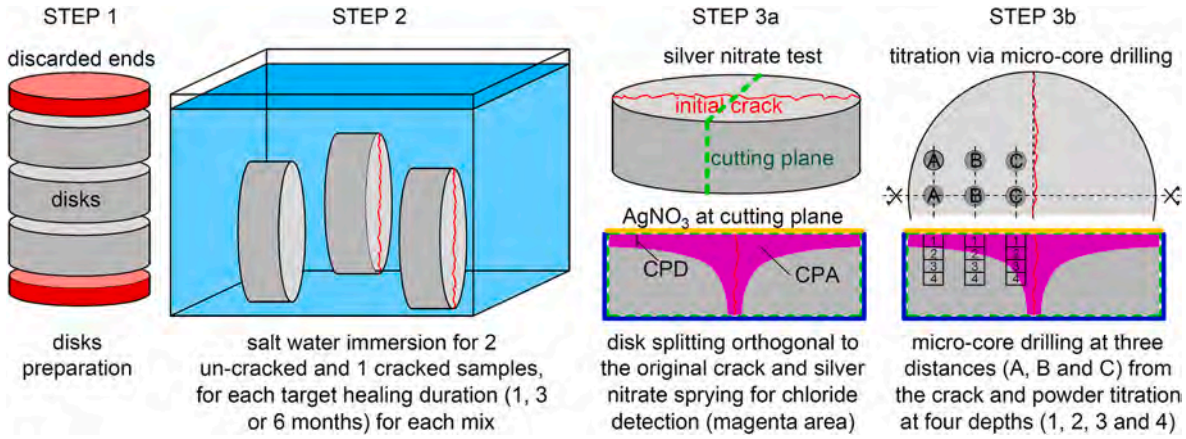

Fig. 2. Disks cut from cylinders (step 1), then stored in salt water (step 2); cutting plane of a disk (green dashed line) for $AgNO_3$ analysis and sketch of the area highlighted by $AgNO_3$ in the cutting surface (in magenta colour) (step 3a) and sketch for titration via micro-core drilling (step 3b). (For interpretation of the references to colour in this figure legend, the reader is referred to the Web version of this article.)

exposed to $AgNO_3$ contained the transverse section of the previous crack, thus allowing to observe the influence of the crack in the diffusion of chlorides orthogonal to crack walls. As sketched in magenta colour in Fig. 2, sprayed silver nitrate highlighted the area with a significant content of chloride. Such region is then quantified via two parameters, the normalized Chloride Penetration Average depth (CPA), and the Chloride Penetration Depth measured far from the crack tip (CPD), as reported in Equations (2a) and (2b):

$$CPA\ [mm] = \frac{area\ of\ the\ region\ highlighted\ by\ AgNO_3}{diameter\ of\ the\ disk} \quad (2a)$$

$$CPD\ [mm] = depth\ of\ the\ region\ highlighted\ by\ AgNO_3 \quad (2b)$$

CPD represents the chlorides penetration depth in un-cracked condition, while CPA takes into account the effect of the crack and thus of crack self-healing.

On the other hand, chemical titration was performed similarly as per BS EN 14629:2007 or RILEM TC 178-TMC, according to a modified procedure conceived for this kind of materials (which are characterized by a large amount of steel fibres).

The procedure starts with drilling micro-cores with a diameter of 10 mm at three different positions parallel to the initial diametrical crack and at three different distances orthogonal to it (A, B and C in step 3b of Fig. 2). As progressively drilled, the material in form of powder was separated at four different equally spaced 5 mm depths, from 0 to 20 mm (1–4 in step 3b of Fig. 2). The 36 determinations obtained for each specimen allowed to "reconstruct" the chloride penetration profiles. Since this latter approach has been adopted by Lab1 and Lab4 only, and the results of one of the two labs can be already found in Ref. [48], this second procedure is not further discussed in the present paper.

2.2.2. *Water permeability recovery on disks*

In each laboratory involved, water permeability test was carried out on each mixture on five concrete disks with nominal dimensions Ø100 × 50 mm, obtained by cutting Ø100 × 280 mm cylinders (Fig. 3). Each disk was *pre-cracked* by splitting at time 0 with a target residual crack width of (100 ± 50) μm after unloading, with the same set-up shown for chloride penetration test (Fig. 1).

Water permeability and crack image analysis were performed at time 0 (just after pre-cracking) and at the three healing periods, 1, 3 and 6 months from pre-cracking. The Index of Crack Sealing was calculated via image analysis at such target periods, in the same way described for chloride penetration test (Equation (1)). During the whole healing period, disks were kept immersed in tap water.

Water permeability test was performed by enforcing a water level of 55 cm above one of the two basis planes of the specimens. This was done by gluing PVC tubes on the top of the disks (orange in Fig. 3) then filled with local tap water. During the test, the water mass flow through the thickness of the disks was monitored for 3 h at different time intervals (namely, 0, 5, 10, 15, 20, 25, 30, 40, 50, 60, 80, 100, 120, 150 and 180 min). A very similar testing procedure has been extensively implemented in Refs. [32,48,57,72], while water under pressure has been implemented in Refs. [69,70].

The indirect permeability index k_t was finally evaluated as the slope of flown-through water volume versus time curves in the range 100–180 min. Before performing the permeability test, the samples were preconditioned by 24 h-drying at 60 °C.

The Index of Permeability Recovery (IPR) was then calculated as

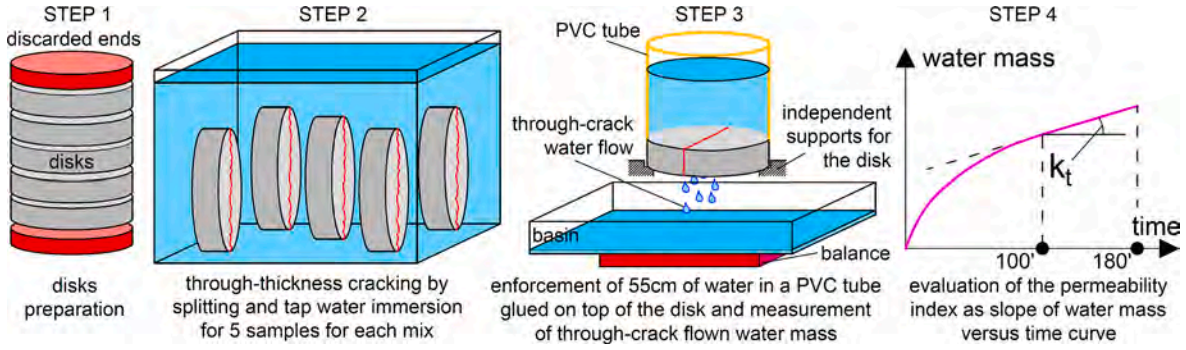

Fig. 3. Disks cut from cylinders (step 1), then stored in tap water (step 2); sketch of the water permeability test setup (step 3) and qualitative plot of water mass flow versus time with the evaluation of k_t coefficient (step 4).

expressed in Equation (3):

$$IPR = 1 - \frac{k_t}{k_{t0}} \tag{3}$$

2.2.3. Strength and stiffness recovery on thin beams

The mechanical recovery triggered by self-healing was assessed via 4-point bending tests on thin beams with nominal dimensions of 25 × 100 × 500 mm^3, with the aim of highlighting the multiple-cracking behaviour in the central region of the specimen. Such behaviour is representative for materials with strain/deflection-hardening response and hardly sizable in 3-point bending test (3PBT).

During the test, the tensile deformation at the bottom side was monitored to measure the target residual strain after unloading. In Fig. 4 the setup adopted at PoliMi is shown and very similar tests setups have been adopted by the other labs.

In order to assess any possible mechanical recovery as a function of the healing period, specimens were re-tested in bending at all the target periods, namely at time 0 (*pre-cracking*), and after 1, 3 and 6 months (*re-cracking*) of healing. At each cracking step (both *pre-cracking* and *re-cracking*) an additional residual strain (after unloading) of 1 ‰ was attained.

At the end of pre-cracking via four-point bending (time 0), at least one crack at the bottom side of each specimen was recorded via digital microscope and image analysis was performed, in the same way discussed for disks. The same was done just before and just after any further re-cracking (at 1, 3 and 6 months from time 0).

For each specimen, the total deformation was then obtained from consecutive σ-COD cycles by translating the σ-COD curves along the x-axis in order to match the first point of the re-cracking (i) with the last point of the previous cracking (i-1), as shown in Fig. 4c and d. This curve has then been compared to the reference one, namely the one related to an un-cracked specimen tested monotonically up to failure at the same time period with the same curing (at 1, 3 and 6 months from time 0).

This testing procedure has been developed in recent years with special reference to UHPFRCC [8,23,32,72,73] which, as mentioned above, is characterized by a signature tensile response usually leading to strain-hardening. This is the reason why 4-PBT is preferred, so to instate a multiple cracking regime which is representative in terms of crack pattern and crack width.

All the beams have been cast, cured and prepared at PoliMi and then shipped to the lab involved, ready to be pre-cracked. In each laboratory and for each mixture composition, 15 specimens were provided, 8 to be tested monotonically up to failure at each reference time (thus 2 specimens at time 0 and 2 after further 1, 3 and 6 months), and 7 to be pre-cracked at time 0, and then re-cracked at 1, 3 and 6 months for self-healing assessment.

Analysing the re-constructed curves of the pre-cracked/re-cracked specimens (as shown in Fig. 4c) and comparing them with the reference one (as shown in Fig. 4d), it is possible to evaluate the mechanical recovery from the translated σ-COD curves by means of the following indexes:

- *Indexes of Stiffness Recovery (ISR)* according to Equations (4a) and (4b):

$$ISR_0\,[-] = \frac{K_c^i - K_s^0}{K_c^0 - K_s^0} \tag{4a}$$

$$ISR_{i-1}[-] = \frac{K_c^i - K_s^{i-1}}{K_c^{i-1} - K_s^{i-1}} \tag{4b}$$

ISR_0 represents the recovery with respect to the pre-cracking cycle (first loading cycle), while ISR_{i-1} represents the recovery with respect to the previous cracking cycle (either pre-cracking or re-cracking cycle). The two indexes are based on the evaluation of initial loading stiffness (K_c^0), first unloading stiffness (K_s^0), (i-1)th unloading stiffness (K_s^{i-1}) and ith re-loading stiffness (K_c^i), as sketched in Fig. 4c. ISR_0 and ISR_{i-1} are evaluated analysing singularly each reconstructed curve.

- *Index of Resistance Recovery (IRR)*, evaluated as expressed in Equation (5):

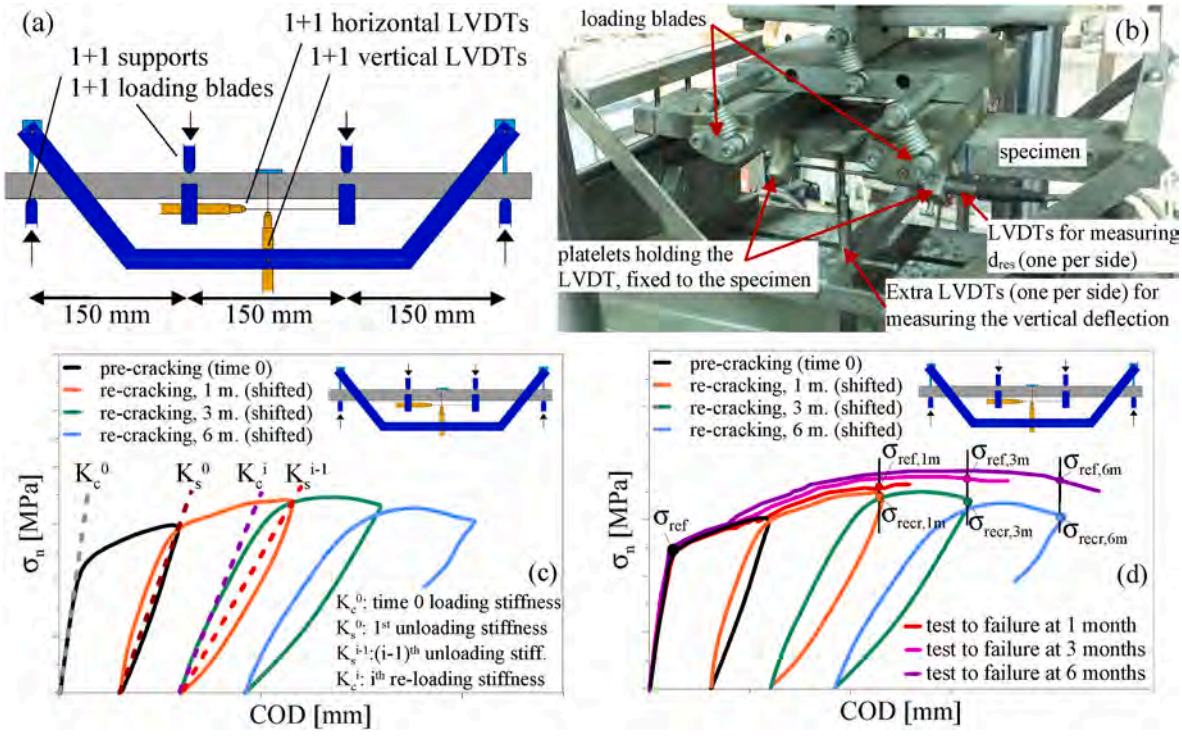

Fig. 4. Scheme (a) and picture (b) of the four-point bending test setup for pre-cracking and re-cracking of thin beams, and evaluation of (c) stiffness recovery and (d) strength recovery indexes.

$$IRR[-] = 1 + \frac{\sigma_{recr,i} - \sigma_{ref,i}}{\sigma_{ref}} \quad (5)$$

The term $\sigma_{recr,i}$ is the stress at unloading at the i^{th} cracking cycle, $\sigma_{ref,i}$ is the stress in the reference curve in correspondence of the same strain of $\sigma_{recr,i}$, and σ_{ref} is the stress in the reference curve as sketched in Fig. 4d. IRR is valuated comparing each reconstructed curve with the reference one.

For all indexes, the value equal to 1 indicates complete recovery of the pristine performance of the specimen in its virgin/previous state. Crack visual inspection was also performed as described for the concrete disks in the previous section, thus allowing to evaluate the Index of Crack Sealing (ICS).

During the whole healing period, disks were kept immersed in tap water without any further pre-conditioning before flexural tests or crack image analysis.

2.3. Specimen production

All the specimens tested by the different laboratories involved in the Round Robin Test were cast and prepared at Politecnico di Milano at the end of 2019, respecting the above-mentioned mixing protocol. For each lab and for each of the two mixtures to be investigated, fifteen small beams (25 × 100 × 500 mm^3) were produced, together with 4 cylinders (D x H = 100 × 280 mm).

It is worth underlining that small beams were produced by casting concrete slabs with a nominal thickness of 25 mm and in-plane dimensions 500 × 1000 mm^2 that were then cut at PoliMi into 20 beam specimens (100 mm wide and 500 mm long). Such procedure has been adopted since it guarantees a better alignment of fibres as compared to the production of single specimens [54,57].

On the other hand, 28 whole cylinders for each mixture have been prepared and cured at Polimi. Four cylinders per mixture were then shipped to each lab involved, the latter one being responsible for cutting the disks and for all the following procedures. By cutting nine 80 mm-thick disks (from 3 out of 4 cylinders) and five 50 mm-thick disks (from 1 out of 4 cylinders), for each mixture, samples for testing chloride penetration and water permeability were obtained, respectively.

Table 3 shows the overall experimental program carried out in this study, while in Table 4, the experimental test type performed in each lab is reported. Finally, Table 5 shows the anonymous identification of the labs involved, together with the correspondent symbol adopted for data and results in Section 3.

Due to CoVID-19 pandemic, specimens were shipped to the participating laboratories just after about one year from casting, in the second half of 2020. This, however, allowed to smooth down any delayed hydration process within concrete, including latent hydraulicity of the slag.

In the complete curing period, specimens were kept in a moist room, with a temperature of 20 °C and R.H. of 90 %.

Table 4
Laboratories involved in RRT4 and correspondent performed tests.

	Chloride penetration	Water permeability	4PBT on thin beams
Polimi	**X** (titration + ICS)	**X**	**X**
UGent	**X** (silver nitr + ICS)	**X**	**X**
UPV	**X** (silver nitr + ICS)	**X**	**X**
LU	**X** (titration + ICS)	**X**	**X**
UoM	**X** (silver nitr + ICS)	**X**	-
TUD	**X** (ICS)	**X**	-
CSIC	-	**X**	-

Table 5
Anonymous identification of laboratories involved in RRT4 and correspondent symbols.

	symbols in the plots	
	w/o admixt.	with admixt.
Lab 1	○	●
Lab 2	▢	■
Lab 3	△	▲
Lab 4	⬦	◆
Lab 5	+	✚
Lab 6	✲	✶
Lab 7	▽	▼
Avg	◑	◐

3. Results and discussion

3.1. Chloride penetration test

At the reference time durations for self-healing assessment, namely at 1, 3 and 6 months from time 0, a triplet of disks (two of which pre-cracked at time 0 and one un-cracked) was split orthogonally to the initial crack and then examined by means of silver nitrate sprayed on it (as sketched in Fig. 2). The region highlighted by silver nitrate is quantified via Chloride Penetration Average depth (CPA) and Chloride Penetration Depth measured far from the crack tip (CPD).

The average variation with time of CPD is reported in Fig. 5a as a function of the healing period. Cracked and un-cracked disks are considered together since CPD is evaluated far from the crack, where its influence on the chloride penetration depth is negligible (thus no sizable difference is expected between cracked and un-cracked specimens). On the other hand, CPA average values are reported in Fig. 5b and c for each healing period differentiating between cracked and un-cracked disks.

Focusing on CPD, it can be observed that, over time, the chloride penetrates less deep into the specimens with crystalline admixture

Table 3
Overall experimental program of RRT4.

Month	Chlorides diffusion *9 specimens*	Water Permeability *5 specimens*	4-P bending in thin beams *15 specimens*
0	• specimens 1 to 6 pre-cracked • specimens 7 to 9 un-cracked • 9 disks immersed in salt water	• 5 specimens pre-cracked • 5 permeability tests done	•7 specimens pre-cracked •2 specimens tested to failure • 6 spec. un-cracked cured as cracked
1	• spec. 1, 2, 7 split and titrated • spec. 3 to 6, 8, 9 kept in salt water	• 5 specimens subjected to permeability test	• 7 specimens re-cracked • 2 spec. un-cracked tested up to failure
3	• spec. 3, 4, 8 split and titrated • spec. 5, 6, 9 kept in salt water	• 5 specimens subjected to permeability test	• 7 specimens re-cracked • 2 spec. un-cracked tested up to failure
6	• spec. 5, 6, 9 split and titrated	• 5 specimens subjected to permeability test	• 7 specimens re-cracked • 2 spec. un-cracked tested up to failure
healing storage **preconditioning**	continuous immersion in salt water (with 33 g/L NaCl) no pre-conditioning before cracking/splitting/titration	continuous immersion in tap water 24 h-drying at 60 °C before permeability test	continuous immersion in tap water no pre-conditioning before flexural testing

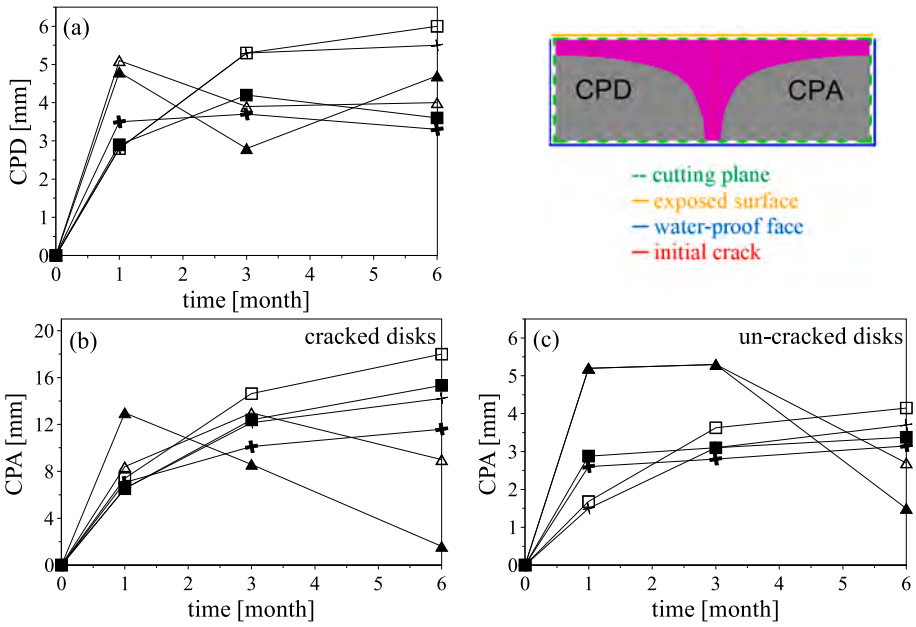

Fig. 5. Average values of CPD for all disks (a) and of CPA for cracked disks (b) and un-cracked disks (c) as functions of self-healing time for the mixtures without and with crystalline admixture.

thanks to the lower porosity of the matrix as fostered by the crystalline admixture [74]. It is worth noting that CPD and CPA in un-cracked specimens provide comparable results (with all data comprised in the range 1.5–6.0 mm), since CPA in un-cracked specimen represents the average penetration depth along the diameter.

The scattering among the results of the three laboratories involved is rather limited in the case of CPD, while it is larger in the case of CPA. This is probably due to the influence of (a) the water-tightness of the lateral faces which affects the penetration of chloride at the edges and of (b) the initial crack width after pre-cracking (which is on average 127, 158 and 130 μm for Lab2, Lab3 and Lab5, respectively, with standard deviations of 35, 95 and 52 μm, respectively).

In all the cases, however, also CPA proves a slightly lower penetration of chlorides into the specimens with crystalline admixture thanks to the lower initial porosity fostered by this admixture [74] and, likely, also to a more effective crack sealing allowed by it. As expected, comparing cracked and un-cracked specimens, it can be observed that CPA is much larger in the former case due to the presence of cracks which allow a significant inlet of chlorides.

Regarding CPA for both cracked and un-cracked disks, the markedly different trend observed at Lab3 with respect to Lab2 and Lab5 in the range 3–6 months of healing has been object of investigation, but a clear explanation has not been identified. Most of the disks used at Lab3 for the characterization at 6 months belonged to the bottom part of the cylinders, where a slightly larger content of fibre and a lower porosity is expected, this probably leading to lower values of chlorides penetration.

Further information can be obtained thanks to the titration as discussed in details in Ref. [48]. It was found that after one-month exposure, in the mixture without crystalline admixture an immediate quite strong penetration of chlorides throughout the crack depth was evident,

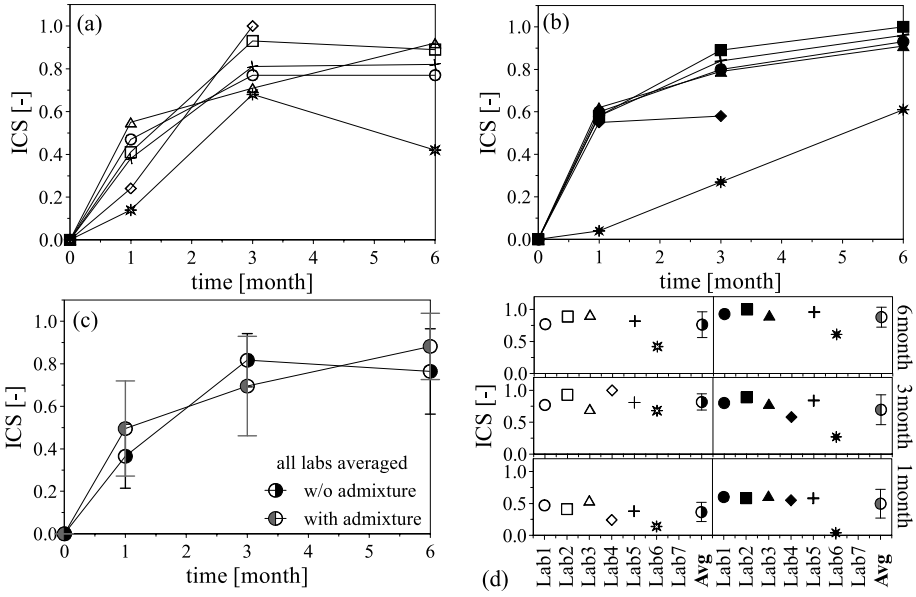

Fig. 6. ICS for the mixtures without (a,d) and with (b,d) crystalline admixture divided per laboratory, and values averaged among all the laboratories (c,d).

whereas a sizably lower trend has been measured for the mix with crystalline admixture. This is likely a consequence of a faster crack sealing in the latter case. For prolonged exposure time up to six months, the penetration of chlorides along the cracked plane continued, in this case the better crack sealing efficacy of the mixture with crystalline admixture being instrumental at reducing the chloride content by about 20–25 %.

Regarding the values of ICS reported in Fig. 6, among five of the six laboratories involved (Lab1, Lab2, Lab3, Lab4 and Lab5) a satisfactory agreement can be observed, both considering singularly each of the two mixtures, and comparing the trend going from the mixture with admixture to the mix without. In general, no significant difference between the mixes with or without crystalline admixture can be observed.

Table 6 shows the initial crack width (averaged for each mix among the 6 cracked specimens) without highlighting specific trends with respect to Fig. 6.

3.2. Water permeability test

Figs. 7 and 8 show the values of the Indexes of Permeability Recovery (IPR) and of Crack Sealing (ICS), respectively, for the two investigated mixtures as functions of the healing time. The values of IPR and ICS plotted represents the average of data obtained from 5 disks, for each concrete mixture at every healing period. Fig. 7a and b and Fig. 8a and b report the results related to the mixtures without and with crystalline admixture, respectively, for each participant, while Figs. 7c and 8c report the average values considering all labs together.

It can be observed that the scattering of the results among the laboratories is less evident in the case of IPR with respect to ICS, since, as also observed in Refs. [48,57], self-healing effectively affects water flow through very narrow cracks when a limited water pressure overhead is considered [69–72]. Nevertheless, the trend shown going from mixture without to mixture with admixture is not very clear, since, in general, the differences between the two species are rather limited. Averaging all data (Fig. 7c), it appears that the introduction of crystalline admixture brings scant benefits in terms of water permeability recovery.

Similar considerations can be extended to ICS, since for Lab1, Lab3 and Lab4 crystalline admixture provides a slightly more efficient recovery, while the opposite is observed by Lab7. On the other hand, no significant difference between the two mixtures has been observed by Lab2, Lab5 and Lab6.

Also in this case, averaging all data (Fig. 8c), it appears that the introduction of crystalline admixture brings no evident benefit in terms of crack sealing. This can be ascribed to the fact that, in some cases (Lab1, Lab2 and Lab6), the obtained average crack openings fall within a range (50–100 μm) for which the autogenous healing capacity of UHPFRCC was systematically and reliably demonstrated able to close the crack, thus shadowing any possible effect of the stimulation by means of crystalline admixtures. This autogenous healing can occur up to several years of age [75].

Table 7 shows the initial crack width (averaged for each mix among the 5 cracked specimens).

3.3. Flexural tests of thin beams: mechanical recovery and crack sealing indexes

As above mentioned, in the quantification of the healing-induced recovery on the mechanical performance, four-point bending test was preferred over three-point bending since the former allows to observe the multiple cracking stage. This, in fact, is the typical response for such kind of cementitious materials thanks to the activation of the crack-bridging effect of steel fibres. The central region of the specimens bordered by the two loading blades experiences constant bending moment and several cracks form in this region (which can be meant as characterized by a constant smeared tensile strain).

This aspect is rather important since it allows to define reference thresholds in terms of strain, rather than in terms of crack width, the latter not being known a priori in structural applications. An interesting range of values of tensile strain is 2.0–2.5 ‰ which comprises the nominal strain related to f_{R1k} and the characteristic yielding strain of common reinforcement bars. In particular, f_{R1k} is the reference residual strength of Fiber-Reinforced Concrete for serviceability conditions (as measured via 3-Point Bending Test) and it is equal to about 2.0 ‰. On the other hand, the characteristic yielding strain of reinforcement bars is equal to about 2.4 ‰ for the most used steel type in Europe (namely B500).

In order to explore such range of tensile strain, the nominal residual value of 1 ‰ at each cracking stage was set in the test programme, thus obtaining 1 ‰ after initial pre-cracking at time 0 and 2 and 3 ‰ after second (at 1 month) and third (at 3 months) re-cracking. Tensile deformation was measured in the tests at the bottom side of the specimen between the supports by displacement transducers across the whole central zone (see also [48]).

For a deeper understanding of the results reported in the following, the distribution of the crack width observed in the specimens after pre-cracking and after each re-cracking is shown in Fig. 9. It plots the percentage of cracks versus the crack width, organized in crack width ranges of 10 μm, for the different observation periods.

The widest range of crack opening was experienced in the tests performed at Lab1, where cracks up to 90–100 μm were observed after the first pre-cracking. On the contrary, at Lab3 most of the cracks belonged to the range 0–30 μm, while an intermediate condition can be highlighted for Lab2 and Lab4. Looking at the medians, however, crack width varies from 0-10 μm (Lab3) to 30–40 μm (Lab1).

For chloride and permeability testing, a 100 μm wide crack was thus set as a target in the pre-cracking phase, since it represents an upper bound for crack width in this kind of UHPFRCC.

The observed difference in median crack width can be ascribed to

Table 6
Average values (w_{avg}) and standard deviations (w_{σ}) of initial crack opening at time 0, for the mixtures without and with crystalline admixture (CA).

	Without CA		With CA	
	w_{avg} [μm]	w_{σ} [μm]	w_{avg} [μm]	w_{σ} [μm]
Lab1	109	±57	62	±22
Lab2	114	±39	140	±26
Lab3	193	±120	124	±50
Lab4	88	±52	76	±76
Lab5	144	±59	117	±46
Lab6	66	±30	71	±21
Lab7	-	-	-	-
Avg	114	±48	95	±35

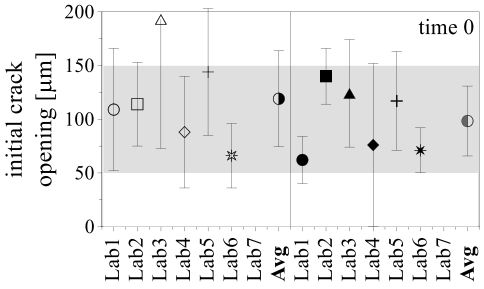

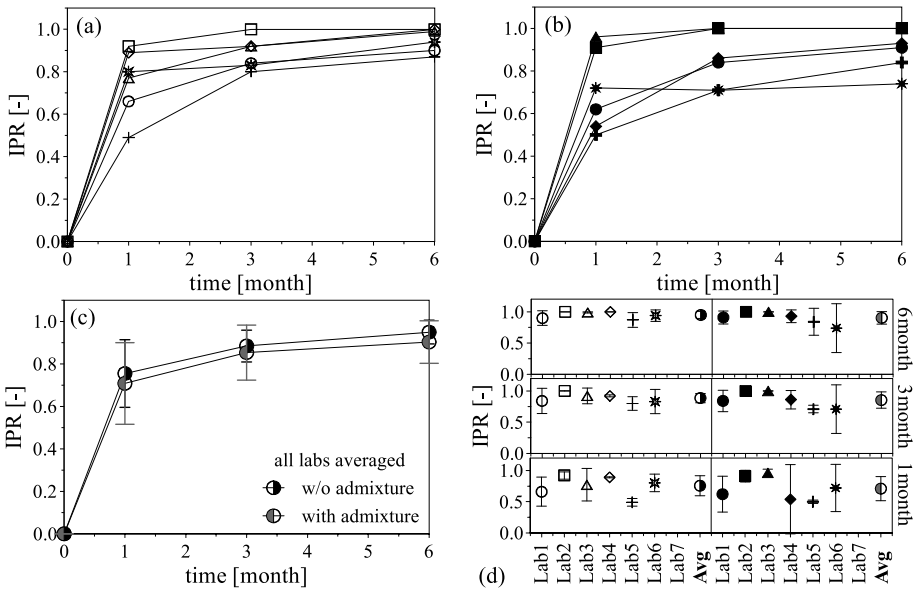

Fig. 7. IPR for the mixtures without (a,d) and with (b,d) crystalline admixture divided per laboratory, and values averaged among all the laboratories (c,d).

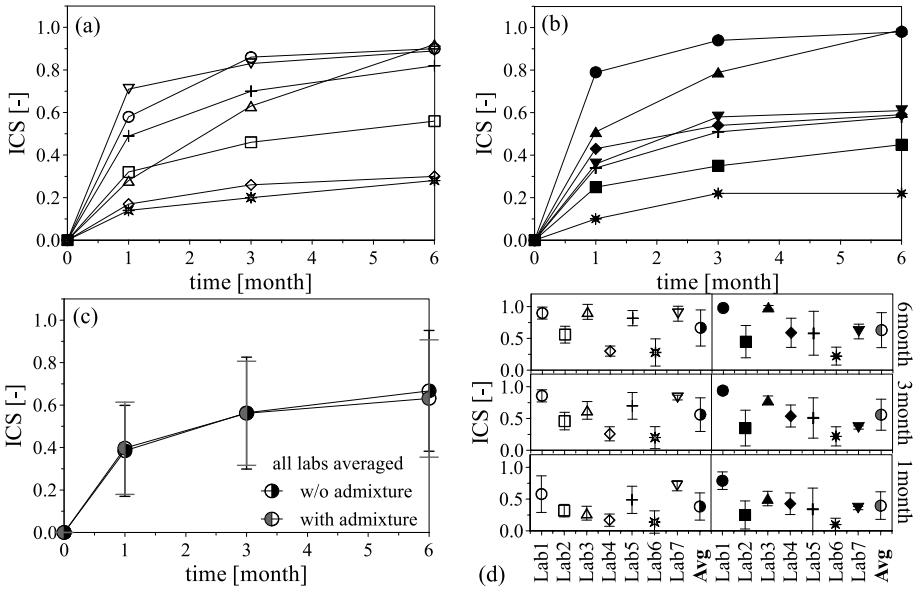

Fig. 8. ICS for the mixtures without (a,d) and with (b,d) crystalline admixture divided per participant, and values averaged among all participants (c,d).

Table 7
Average values (w_{avg}) and standard deviations (w_σ) of initial crack opening at time 0, for the mixtures without and with crystalline admixture (CA).

	Without CA		With CA	
	w_{avg} [μm]	w_σ [μm]	w_{avg} [μm]	w_σ [μm]
Lab1	116	±82	54	±34
Lab2	100	±14	114	±23
Lab3	137	±35	192	±77
Lab4	185	±55	181	±150
Lab5	115	±66	230	±146
Lab6	72	±20	86	±40
Lab7	605	±435	441	±436
Avg	190	±186	185	±129

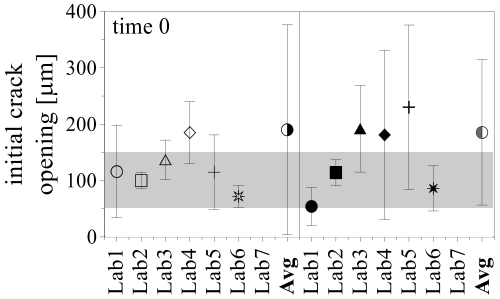

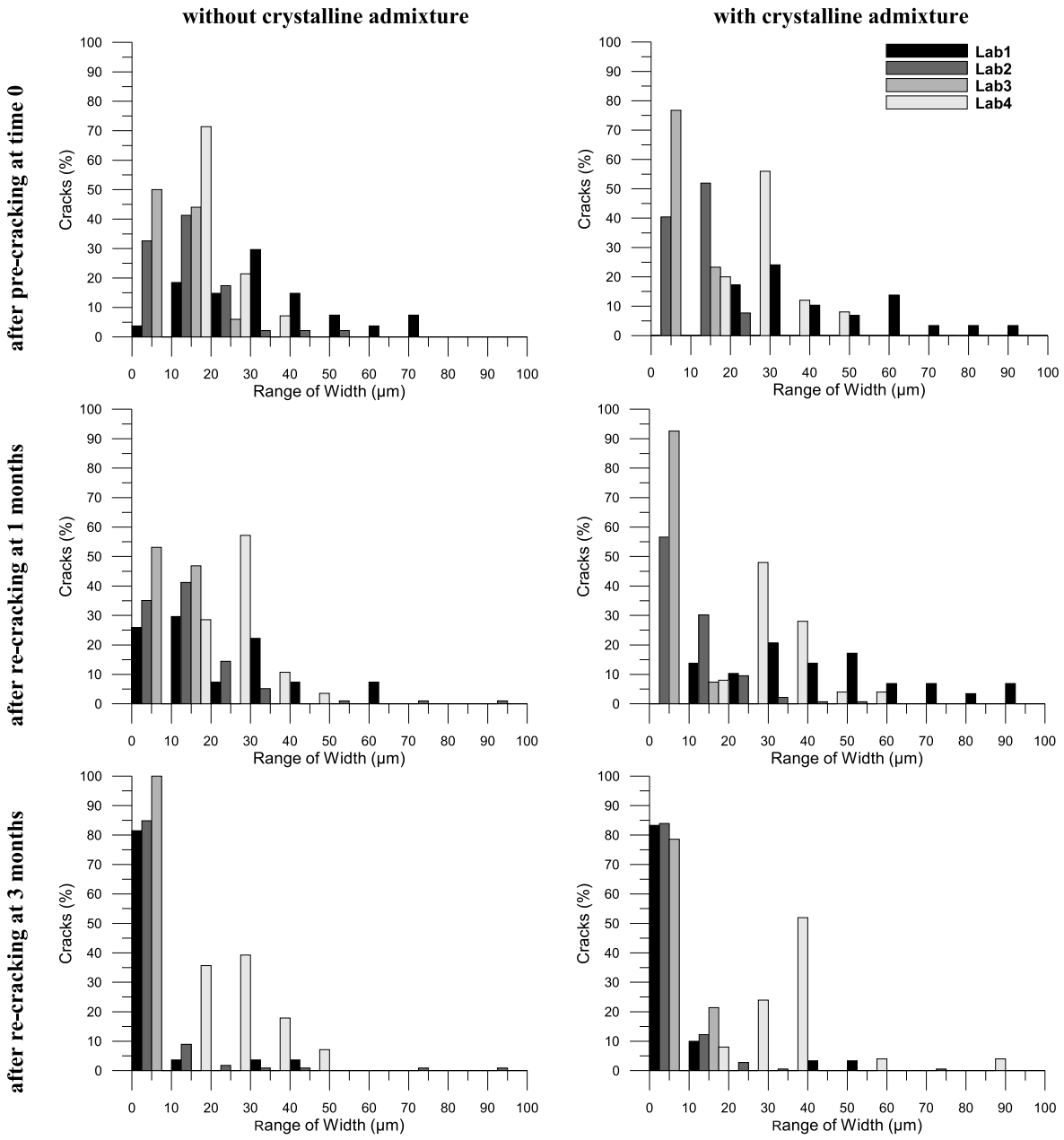

Fig. 9. Crack width distribution at each cracking stage for mixture without and with crystalline admixture, differentiating among laboratories.

slightly inevitable variations among the batches in terms of fibre distribution/orientation which can lead to differences in terms of average distance among cracks (thus influencing the number of cracks and their average opening). These differences in terms of initial crack width should be taken into account when discussing the results regarding self-healing indexes.

Fig. 10 shows the Index of Stiffness Recovery with respect to pre-cracking (ISR_0), differentiated per each participant in Fig. 10a and b, and averaging all the data in Fig. 10c, for the mixtures without and with admixture. The same scheme is followed in Fig. 11 for the Index of Stiffness Recovery with respect to previous re-cracking (ISR_{i-1}).

Focusing on the ISR_0 index, a rather good agreement can be observed for the results of Lab1 and Lab2, whereas the results from Lab4 lead to much lower values (even though no evident differences in the crack width distribution or curing conditions have been noticed). On the opposite, Lab3 observed significantly higher values at 3 and 6 months of healing. This last outcome can be ascribed to a preferential localization of fibres in the bottom part of the specimen (this being responsible for initial cracks characterized by reduced interspace and narrow width), thus leading to a rather steep slope in the reloading curve for limited stress level (up to about 25 % of tensile strength), with a consequent higher observed recovery in terms of stiffness.

Considering the results from Lab1 and Lab2, crystalline admixture yields a more significant healing for all the curing durations, while looking at the averaged values among all participants a clear trend is not evident.

Very similar considerations can be made regarding ISR_{i-1} index, since Lab1 and Lab2 provide results in good agreement, while Lab4 at 1 month provides lower values. On the contrary, Lab4 values at 3 and 6 months are more aligned with the other universities. Also in this case, considering the averaged values among all participants, crystalline admixture appears to have no significant effect on the healing-induced recovery of the mechanical performance.

In order to conclude the analysis on the mechanical healing-related

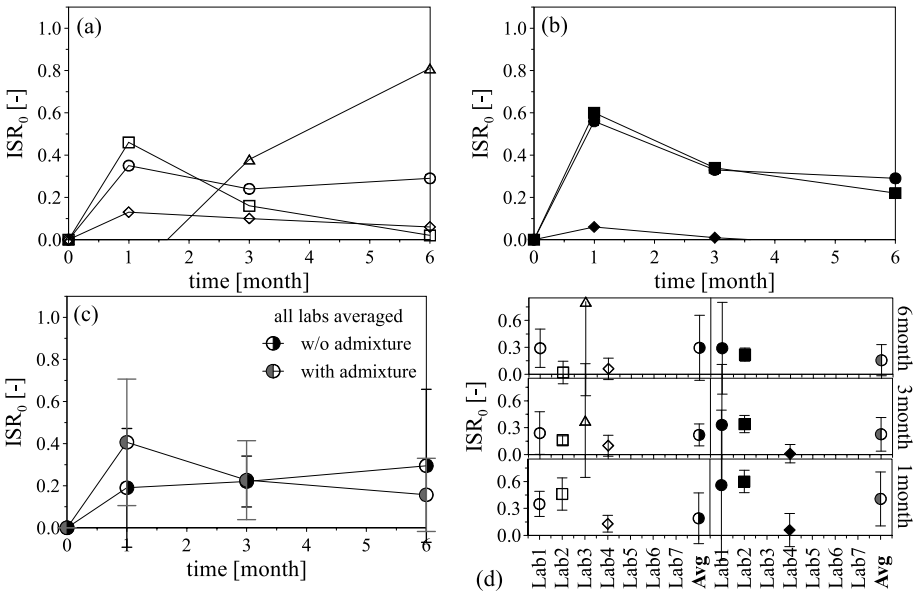

Fig. 10. ISR_0 for the mixtures without (a,d) and with (b,d) crystalline admixture divided per laboratory, and values averaged among all the laboratories (c,d).

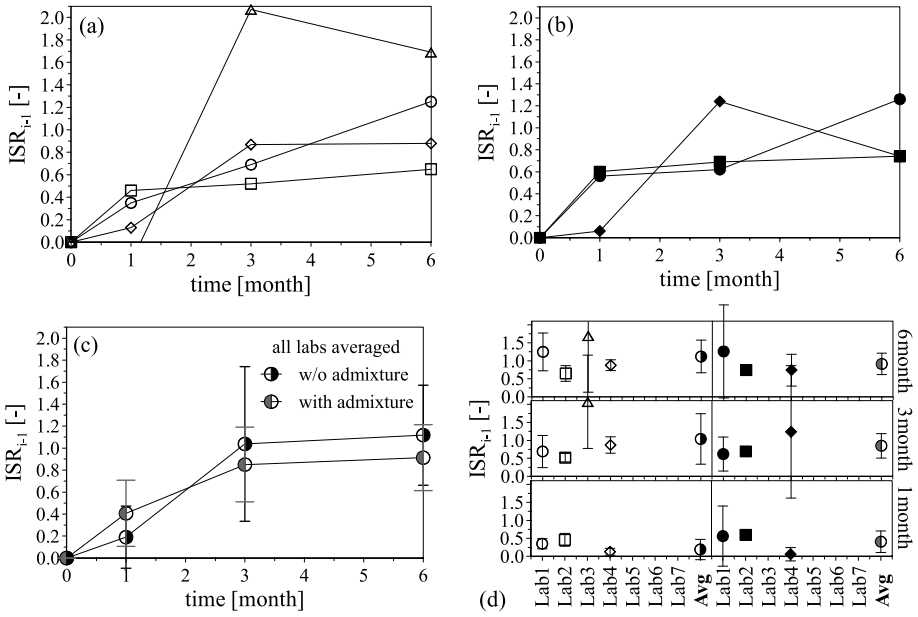

Fig. 11. ISR_{i-1} for the mixtures without (a,d) and with (b,d) crystalline admixture divided per laboratory, and values averaged among all the laboratories (c,d).

indexes, Fig. 12 shows the Index of Resistance Recovery (IRR), differentiating for each laboratory in Fig. 12a and b, and averaging all the data in Fig. 12c, for the mixture without and with admixture. The results related to the mixture without admixture are quite scattered, while for the mixture with admixture a higher repeatability can be highlighted. It is interesting to observe that for Lab1 and Lab2, higher values of recovery are observed for the mixture with crystalline admixture, while an opposite trend yields from the results by Lab3. Averaging all the results in Fig. 12c, therefore, leads to similar performance of the mixtures with and without crystalline admixture.

Finally, Fig. 13 shows the index of crack sealing (ICS), differentiating for each laboratory in Fig. 13a and b, and averaging all the data in Fig. 13c, for the mixture without and with admixture.

It is worth noting that the dataset of cracks is much larger than in the case of the disks used for chloride penetration test and for permeability tests, since in each of the small beams subjected to bending test several cracks have been formed. It can be observed that the results of Lab1, Lab2 and Lab3 are in rather satisfactory agreement for both mixtures.

On the opposite, far lower values of ICS have been assessed at Lab4 (even though no evident differences in the crack width distribution or curing conditions were noticed) with a better performance provided by the mix without admixture. Averaging the data coming from all the laboratories, it can be seen that the differences between both mixtures is not significant also in the case of ICS.

As highlighted in the case of water permeability, the limited differences between the two mixtures can be ascribed to the fact that the autogenous healing capacity of UHPFRCC is rather effective, thus smoothing down any possible effect of the stimulation by means of crystalline admixtures (see also [48]).

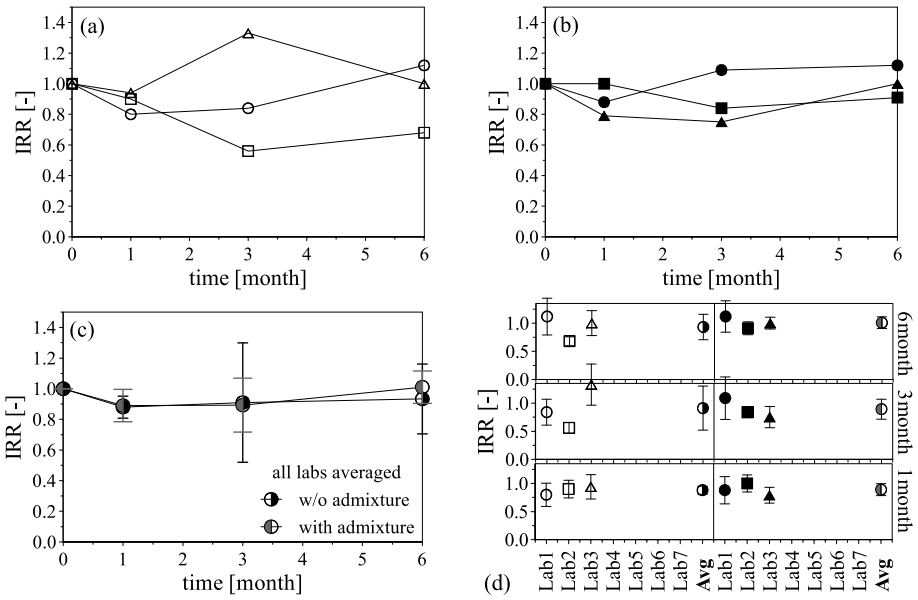

Fig. 12. IRR for the mixtures without (a,d) and with (b,d) crystalline admixture divided per laboratory, and values averaged among all the laboratories (c,d).

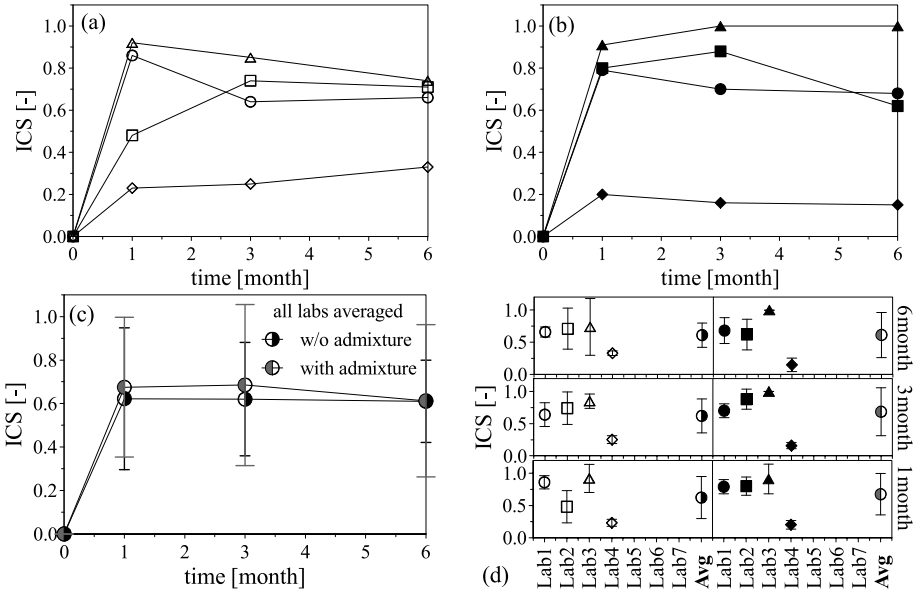

Fig. 13. ICS for the mixtures without (a,d) and with (b,d) crystalline admixture divided per laboratory, and values averaged among all the laboratories (c,d).

3.4. Considerations about the consistency of self-healing indexes

In Table 8 the averaged values μ of all the self-healing indexes are reported for the mixture without and with crystalline admixture together with the coefficient of variation CoV = σ/μ (the latter expressed as a percentage). Average values and coefficients of variation have been calculated considering the population of data represented by the set of average values from each laboratory.

Table 8 allows to preliminary assess the dispersion of the average data coming from different laboratories. Coefficient of variation, in fact, has been also classified as - 1 - *very good* ($0 \leq$ Cov ≤ 10 %, dark green in the table), - 2 - *good* ($10 <$ Cov ≤ 20 %, green), - 3 - *acceptable* ($20 \leq$ Cov < 30 %, light green), - 4 - *poor* ($30 <$ Cov ≤ 40 %, yellow), - 5 - *very poor* ($40 <$ Cov ≤ 50 %, orange), and - 6 - *unacceptable* (Cov > 50 %, red). Once assigned the class for each index, for all the healing periods and for the two mixtures, the average class associated to each of the 10 indexes has been calculated.

If the average class is in the ranges 1–2, the robustness of the index is considered *high*, if it is in the range 3–4, it is considered *medium*, otherwise it is considered *low* or *insufficient*. In the following, the robustness is considered *insufficient* if the average class is larger than 5.5. This corresponds to the case in which, in at least one half of the healing periods, the normalized standard deviation is larger than 50 %. According to such approach the only index to be classified as unreliable is ISR_0.

3.5. Considerations about statistical analyses within a standard-oriented framework

The sizable amount of data related to crack-sealing allows for a statistical analysis aimed at possibly shaping a standard-oriented approach for taking into account self-healing in the design of concrete structures. In particular, while the datasets related to indexes CPD, CPA, IPR, ISR and IRR are limited (since each specimen is associated to a

Table 8
Average values (μ) and standard deviations (σ) of all healing indexes for the two mixtures, in the form μ/± CoV. (CoV classes: (1) = 0-10%, (2) = 10-20%, (3) = 20-30%, (4) = 30-40%, (5) = 40-50%, (6) = >50%).

month	mixture without crystalline admixture									
	chloride penetration				water permeability		flexural tests on thin beams			
	CPD [mm]/[%]	CPAcr [mm]/[%]	CPAun [mm]/[%]	ICS [-]/[%]	IPR [-]/[%]	ICS [-]/[%]	ISR_0 [-]/[%]	ISR_{i-1} [-]/[%]	IRR [-]/[%]	ICS [-]/[%]
0	0	0	0	0	0	0	0	0	1	0
1	3.57/±37	7.45/±12	2.79/±75	0.37/±41	0.76/±21	0.38/±56	0.19/±149	0.19/±149	0.88/±8	0.62/±52
3	4.83/±17	13.26/±10	4.01/±29	0.82/±15	0.89/±8	0.56/±47	0.22/±55	1.04/±68	0.91/±43	0.62/±42
6	5.17/±20	13.74/±33	3.52/±21	0.76/±26	0.95/±6	0.67/±43	0.30/±123	1.12/±41	0.93/±24	0.61/±31

month	mixture with crystalline admixture									
	chloride penetration				water permeability		flexural tests on thin beams			
	CPD [mm]/[%]	CPAcr [mm]/[%]	CPAun [mm]/[%]	ICS [-]/[%]	IPR [-]/[%]	ICS [-]/[%]	ISR_0 [-]/[%]	ISR_{i-1} [-]/[%]	IRR [-]/[%]	ICS [-]/[%]
0	0	0	0	0	0	0	0	0	1	0
1	3.73/±26	8.85/±41	3.56/±40	0.50/±45	0.71/±27	0.40/±55	0.41/±74	0.41/±74	0.89/±12	0.68/±48
3	3.57/±20	10.36/±18	3.73/±37	0.70/±34	0.85/±15	0.56/±44	0.23/±83	0.85/±40	0.89/±20	0.69/±54
6	3.87/±19	9.51/±75	2.68/±38	0.88/±18	0.90/±11	0.63/±44	0.16/±111	0.91/±33	1.01/±10	0.61/±57
eval.	medium	medium	medium	medium	high	low	insuff.	low	medium	low

single value), ICS in thin beams subjected to 4-Point Bending is evaluated for several cracks for each specimen (since multiple cracking is observed in such case). On the other hand, for chloride penetration and permeability on disks, one single value of ICS is associated to each specimen, since in those tests pre-cracking was performed via splitting and a single crack has been observed in the disks. For this reason, a statistical analysis has been performed only on the ICS index related to thin beams, by assuming a Gaussian distribution of the results.

In Fig. 14, the values of ICS for every crack observed in thin beams are shown, divided for participating laboratory and for mixtures without and with crystalline admixture. First of all, it can be highlighted that a significant difference in terms of crack opening is observable among the laboratories, even though the majority of cracks has a width smaller than 50 μm for all the partners.

Despite that for Lab1 cracks up to 100 μm can be observed, while no crack larger than 30 μm was observed by Lab3, in the whole the crack ranges investigated by the different participants appear to be quite consistent. However, a large scatter in the values of ICS has still been observed.

Lab3 shows the highest repeatability with very high values of ICS, mostly indicating perfect recovery already after 1-month healing. On the opposite, Lab4 shows the lowest values of healing, with a good consistency of the results, since most of the results are in the range 5–35 %. Finally, Lab1 and Lab2 observed a sizably larger dispersion of data. As already highlighted in the previous section, however, the final average values of ICS (averaged for each healing period) are rather in agreement among Lab1, Lab2 and Lab3, while they are significantly lower in the case of Lab4 (see Fig. 13).

In order to further investigate possible relationships between ICS and crack width, linear regression algorithms have been applied to the presented dataset. Considering the results related to a single laboratory, a given healing duration (0–1 months, 1–3 months or 3–6 months) and one UHPFRCC mixture, the x axis representing the crack width has been discretized in 10 μm-wide ranges. Within each of them, all values of ICS associated to the crack-width falling in the range have been averaged, so to define a unique value of ICS. For the same set, the standard variation has been estimated.

Triangular symbols in Fig. 15 show averaged values of ICS observed at Lab1, differentiating for the two mixtures and the three healing periods. In the same plot, the continuous line represents the regression line associated to the average values. On the opposite, the dashed line represents the regression curve of the characteristic values, where "characteristic values" refer to the 5^{th} percentile, namely the value of ICS which is overcome by 95% of cracks with a width falling in the given range.

It is worth noting that average regression line and characteristic regression line are parallel since a common standard deviation has been defined for all crack width ranges, calculated as a weighted average among all standard deviations related to the different crack-width ranges. This has been carried out differentiating for the two mixtures and for the three healing periods. Such approach has been followed in order to define the characteristic values also in crack-width ranges in which the amount of data was too limited for a good estimation of standard deviation. Characteristic values have been evaluated assuming a Gaussian distribution of the data.

Regression lines allow to possibly highlight trends in the ICS with respect to the initial crack width. Starting from the results by Lab1, it appears as ICS seems almost independent from the crack width. On the contrary, it could be expected that ICS decreases with the initial crack width due to the increased difficulty in sealing larger cracks. It should be noted, however, that the overall range of crack width herein studied is associated to very small cracks hardly larger than 80 μm, hence it can be considered reasonable that the ICS is not significantly affected by initial crack width. Such outcome is confirmed by Lab3 for very small cracks (<20 μm, see Fig. 17), while a different trend has been observed in Lab2 (Fig. 16) and Lab4 (Fig. 18).

In particular, in Lab2, a strong dependence of ICS on initial crack width can be detected with clear trends in the healing periods 0–1 months and 1–3 months and more scattered data in the period 3–6 months. From the results, it can be stated that no crack sealing can be expected for a crack-width larger than 100 μm even for long healing durations.

Finally, Fig. 19 reports the regression lines obtained by considering the results of all participants together. An intermediate trend between Lab1 and Lab2 can be observed, also because of the larger dataset provided by these two laboratories. In Fig. 19, however, a sizable scattering of data is noted which decreases the reliability of the linear regression in matching the experimental data.

On the other hand, the linear regression represents an easy tool in taking into account *crack healability*, meant as the capability of sealing a crack dependently on the initial crack width. Diagrams of *crack healability* could potentially be used in the design at the Service Limit State (SLS) of structures made of UHPC, with or without ordinary reinforcement. If a linear ICS versus crack-width behaviour is assumed, *crack healability* can be expressed by two parameters only. In Table 9, for example, the two parameters are chosen to be the expected values of ICS

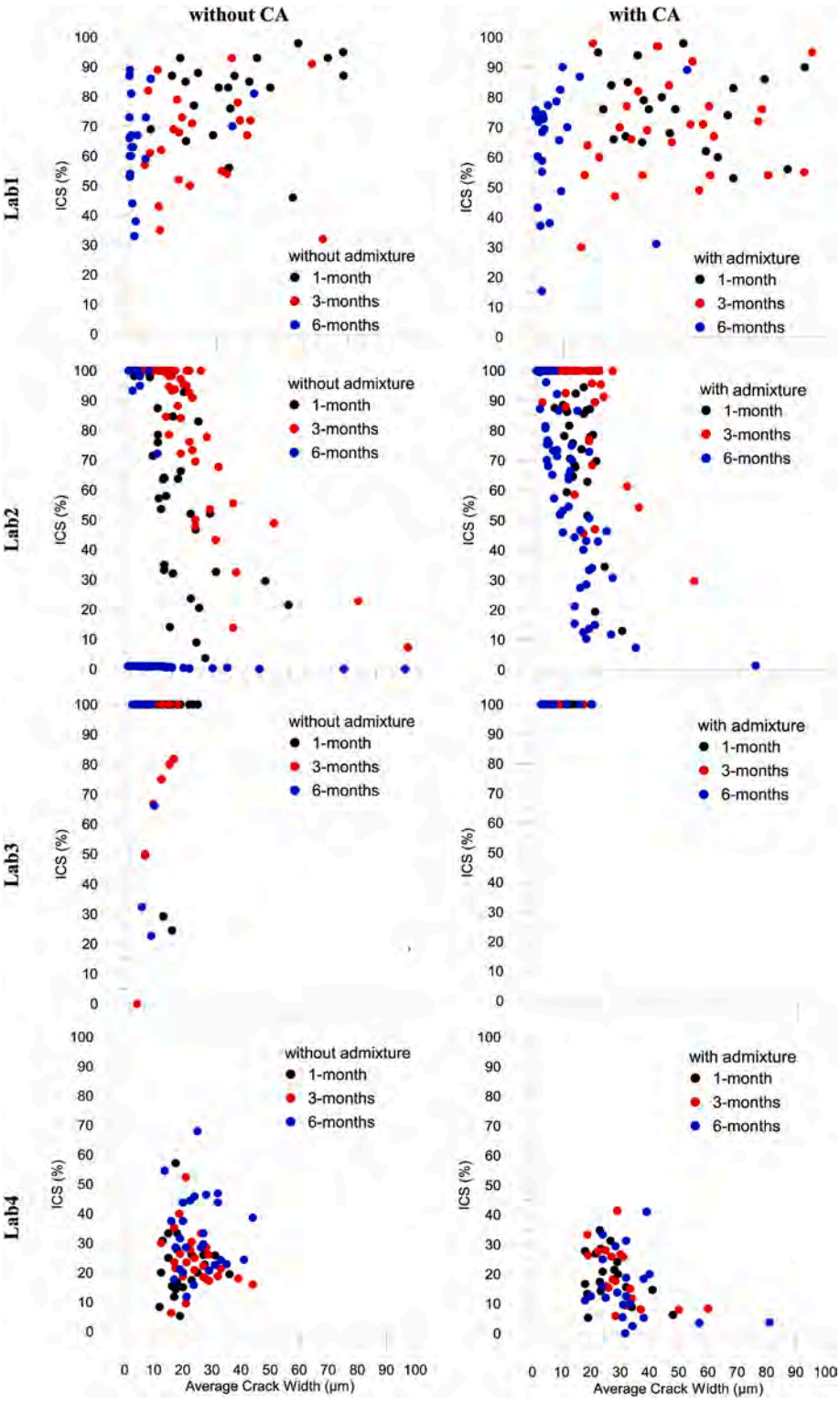

Fig. 14. ICS for the mixtures without and with crystalline admixutre (CA), divided by laboratory.

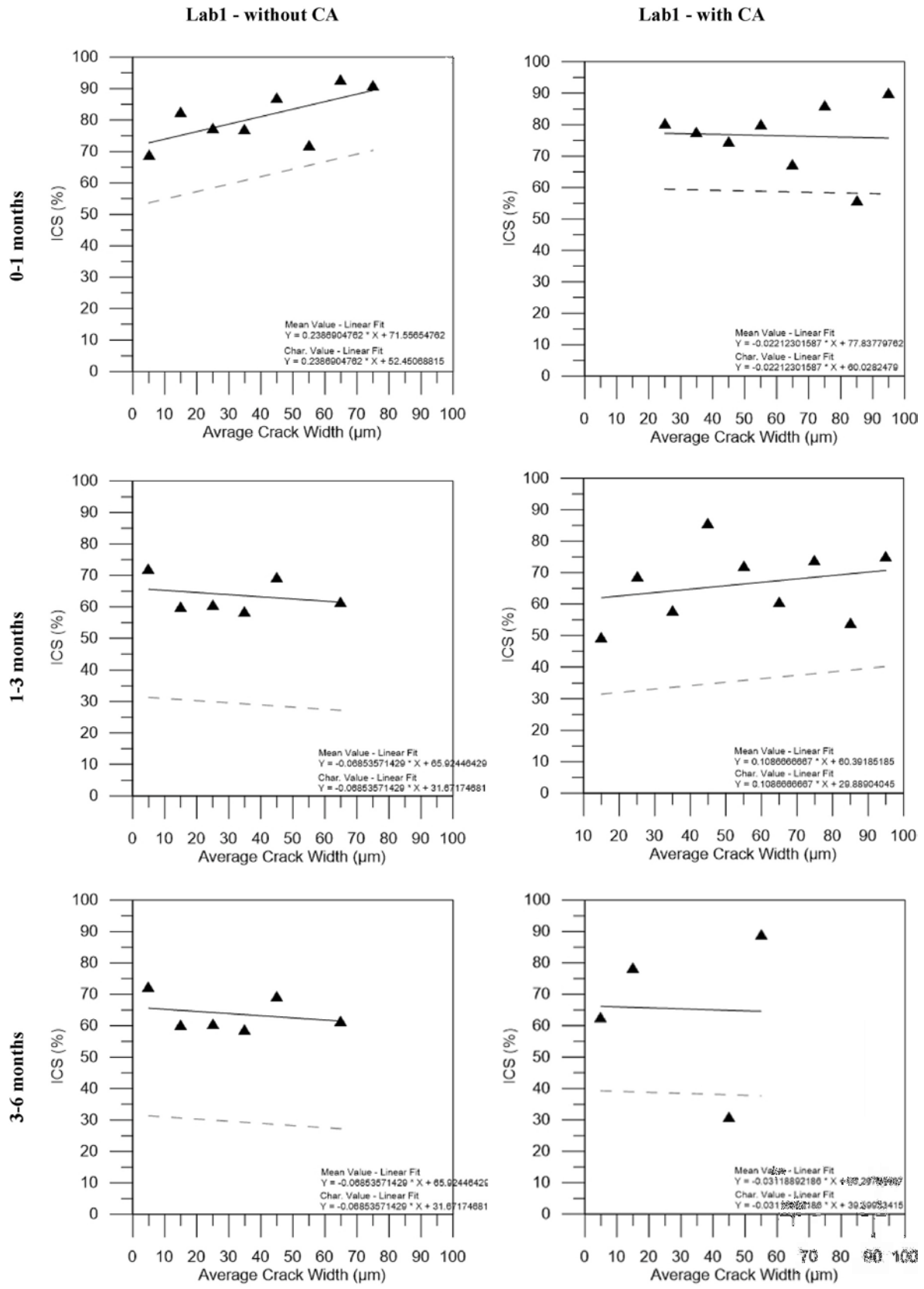

Fig. 15. Lab1: Average values of ICS for the mixtures without and with crystalline admixture (CA) for the different healing periods and regression lines associated to average and characteristic values.

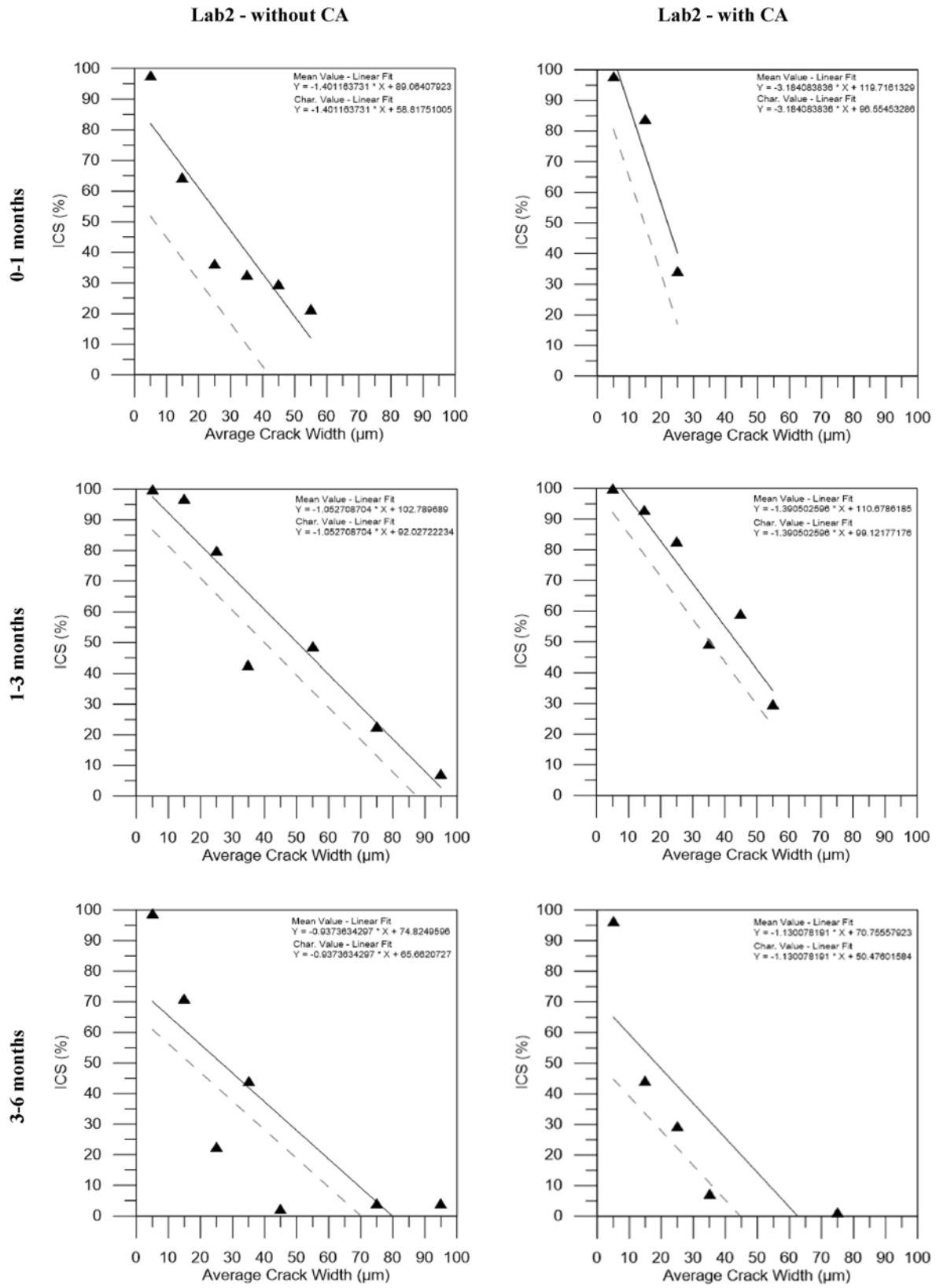

Fig. 16. Lab2: Average values of ICS for the mixtures without and with crystalline admixture (CA) for the different healing periods and regression lines associated to average and characteristic values.

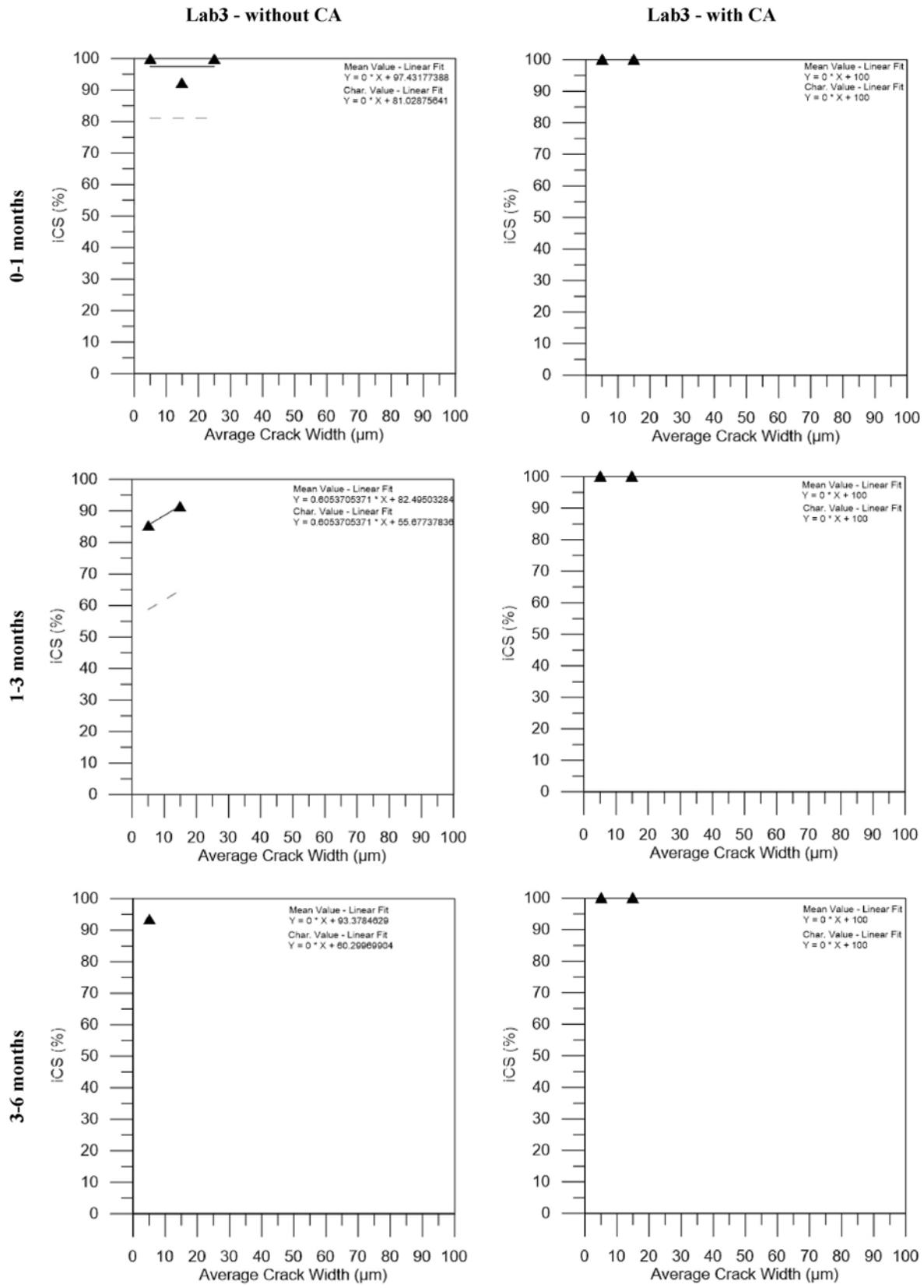

Fig. 17. Lab3: Average values of ICS for the mixtures without and with crystalline admixture (CA) for the different healing periods and regression lines associated to average and characteristic values.

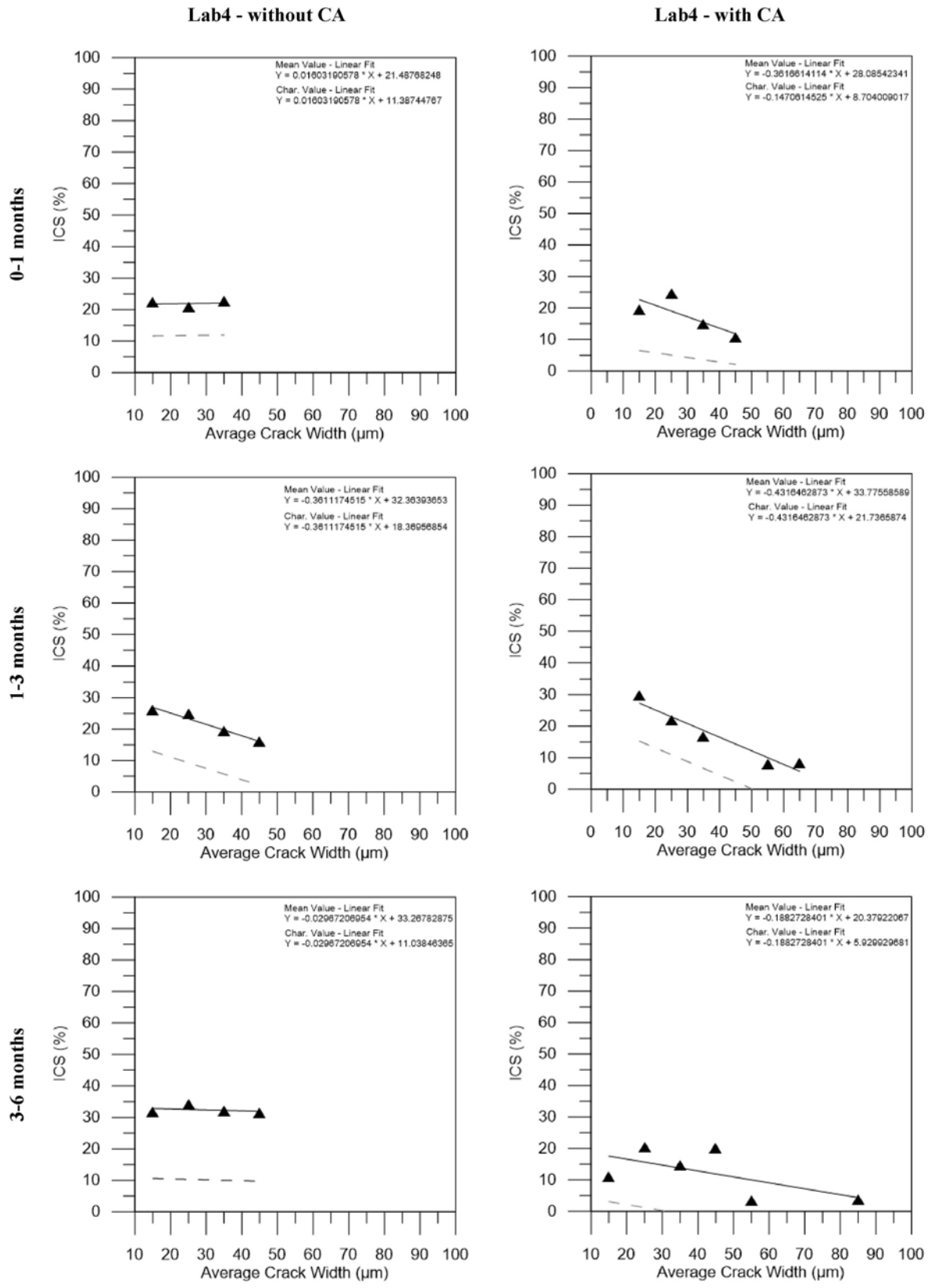

Fig. 18. Lab4: Average values of ICS for the mixtures without and with crystalline admixture (CA) for the different healing periods and regression lines associated to average and characteristic values.

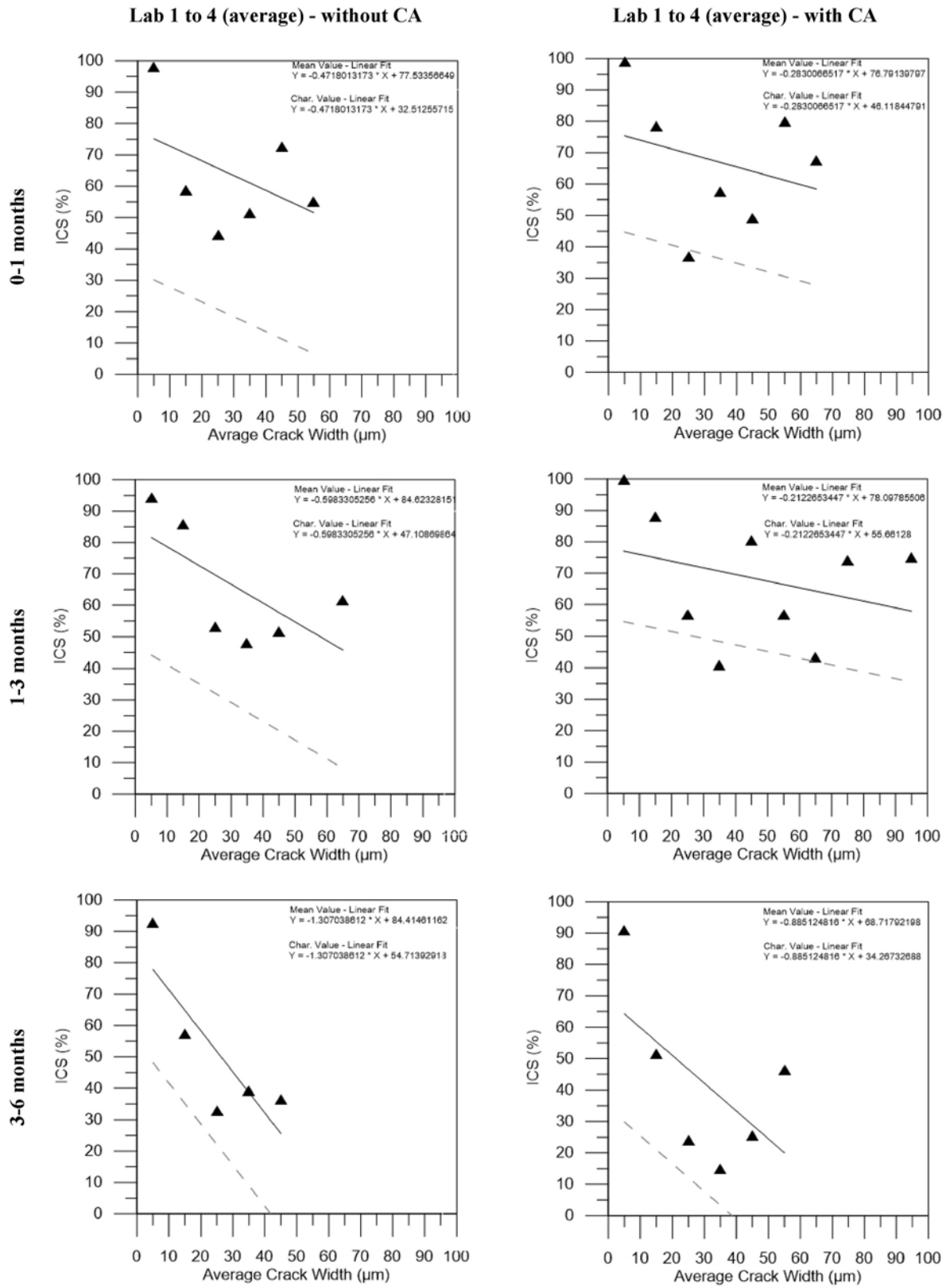

Fig. 19. Lab1, Lab2, Lab3, Lab4: Average values of ICS for the mixtures without and with crystalline admixture (CA) for the different healing periods and regression lines associated to average and characteristic values.

for the two reference crack-widths of 30 and 50 μm. Table 9 highlights that crystalline admixture (CA) leads to higher values of healing practically for all healing durations.

In some cases, Table 9 shows decreasing values of ICS with the healing time due to the repeated cracking (previously referred to as *re-cracking*) performed at the beginning of each period (thus at 1 and 3

Table 9
Expected average values of ICS at 30 and 50 μm, according to statistical analysis, for the mixtures without and with crystalline admixture (CA).

crack width [mm]	0–1 months		1–3 months		3–6 months	
	W/O CA	With CA	W/O CA	With CA	W/O CA	With CA
30 μm	0.63	0.68	0.67	0.72	0.45	0.42
50 μm	0.54	0.63	0.55	0.67	0.19	0.25

months) in small beams under bending. Repeated cracking lead to partially re-opening previously healed cracks in order to reproduce realistic structural cases subjected to variable loads.

4. Conclusions

The present paper has reported the main results yielded by the inter-laboratory test campaign performed on Ultra High-Performance Fibre-Reinforced Cementitious Composites (UHPFRCCs) organized under the umbrella of the COST Action CA15202 SARCOS (Self-healing As prevention Repair of COncrete Structures). The major objective of the campaign was to discuss, in terms of repeatability and consistency, a multi-performance methodology for self-healing assessment in UHPFRCCs.

The multi-performance approach has been conceived to thoroughly investigate the effect of self-healing on both durability and mechanical responses of concrete and concrete structures, having in mind possible real applications of UHPFRCCs.

The experimental procedure is based on three test setups, mostly based on quite established experimental procedures adopted in the research community active on the topic. In particular, the three tests herein implemented are: (1) chloride penetration test on pre-cracked disks, (2) water permeability test on pre-cracked disks and (3) repeated 4-point flexural test on thin beams.

The first test is meant to provide information related to the penetration rate of chloride, the second one to investigate the ability of cracks to recover water-tightness thanks to crack-sealing, while the third one aims at assessing the mechanical performance recovery in terms of strength and stiffness. This latter entails not only the capability of sealing cracks, but also the ability to maintain them closed under applied tension, thanks to crack filling and fibre-matrix bond improvement.

Two UHPFRCC mixtures have been studied, both containing 1.5 % by volume of steel fibres, while just in one of the two a crystalline admixture has been added as a healing promoter. Self-healing has been quantified through a set of suitably defined indexes which also allowed a cross-comparison of results among different tests.

On the base of the data collected from all the laboratories involved and their comparison, the following conclusions can be drawn:

- The test on water permeability is the one showing the highest repeatability, even more when considering that 6 of the 7 working groups performed this test. A rather rapid and efficient recovery of water tightness has been observed already after one month of healing. Despite of the overall repeatability of the results, the differences between the average curves related to the two mixes is comparable with data scattering, thus not allowing to clearly highlight the role played by crystalline admixture.
- The indexes linked to chloride penetration (measured via silver nitrate) also proved a good agreement among the laboratories, even though just three working groups participated to this task. Among the three parameters, Crack Penetration Depth – CPD, Crack Penetration Average depth – CPA on un-cracked disks and CPA on cracked disks, the first and the second ones proved to be analogous. The former resulted to be more consistent and repeatable than the second, thus suggesting that CPA on un-cracked disks could be removed from a possible panel of main healing-related parameters.
- Regarding the healing-related mechanical indexes, the one related to resistance recovery (IRR) resulted to be the most robust one. Far larger scattering was observed for the indexes linked to stiffness, this being probably due to its more complex evaluation with respect to the others.
- Despite its apparent simplicity, the index of surface-crack healing or crack sealing (ICS), based on visual inspection of cracks surface before and after healing, showed a sizable scattering among the laboratories. This can be partly attributed to differences in the initial crack opening. However, this is still under scrutiny, since such parameter is one of the most widely used in the research community for assessing self-healing extent on cementitious materials.
- Focusing on the behaviour of the two UHPFRCCs and the potential positive role of the crystalline admixture as a stimulator of autogenous healing, the scattering of the results related to different laboratories made it difficult to clearly highlight its benefits. Despite that, a faster and less scattered healing was observed in some cases, irrespective of the test and of the testing laboratory. This outcome can also be attributed to the fact that, thanks to the presence of a significant amount of anhydrous particles and the very narrow cracks generated by multiple cracking, autogenous healing in UHPFRCC is particularly efficient. This smooths down the beneficial role played by crystalline admixture in self-healing processes. Such aspect, together with the mentioned scattering among laboratories' data, did not allow to properly assess a difference between the two mixtures.
- According to the discussion about data consistency as reported in Section 3.4, all the indexes appear to be satisfactorily consistent, except for the index of stiffness recovery, whose variation among laboratories resulted to be excessively high.
- A statistical analysis was performed on the widest dataset which was related to the index of crack-sealing (ICS) in thin beams (since multiple cracking in such specimens enabled the evaluation of dozens of values for each laboratory). The significance of the concept of "*crack-width healability*" coming from the correlation of self-healing recovery and initial crack width was highlighted. Such view is expected to push self-healing concepts within a design-oriented framework even though further efforts should be made to increase the overall confidence of the approach.

The preliminary statistical analysis of the data, together with the concept of "*crack-width healability*", can be considered as a first step in the direction of incorporating self-healing concepts into code-based design approaches. This includes a future perspective of systematically implementing defined meta-analysis algorithms, which, by managing and processing significant amounts of data from the available literature, will also allow to provide confidence ranges for the proposed correlations.

It is worth noting that, despite a multi-performance approach should be preferred for the assessment of self-healing capability in UHPFRCCs (according to the specific structural application), for initial material screening a single reference test could be adopted. For the sake of simplicity, the index of crack sealing measured on cracked disks appears to be the most suitable. On the other hand, for a comprehensive characterization of the materials towards typical structural applications, flexural testing (even in combination with chloride penetration on disks) appears to be the most meaningful. Finally, water permeability test can be considered for hydraulic applications as basins, ducts or containing walls/linings under the water table.

Declaration of competing interest

The authors declare that they have no known competing financial interests or personal relationships that could have appeared to influence the work reported in this paper

Data availability

Data will be made available on request.

Acknowledgments

The round robin activity reported in this paper has been performed in the framework of the COST Action CA 15202 "SARCOS" (Self-healing As prevention Repair of COncrete Structures, http://www.sarcos.enq.cam.ac.uk). The production of the material and the inter-laboratory comparison were also supported by the ReSHEALience project (Rethinking coastal defence and Green-energy Service infrastructures through enHancEd-durAbiLity high-performance cement-based materials) which has received funding from the European Union's Horizon 2020 research and innovation program under grant agreement No 760824 (www.uhdc.eu).

References

[1] Healcon, Self-healing Concrete to Create Durable and Sustainable Concrete Structures, University of Gent, Grant Agreement ID 309451, 2013.
[2] M4L, Materials for Life (M4L): Biomimetic Multi-Scale Damage Immunity for Construction Materials, Cardiff University. EPSRC (Engineering and Physical Sciences Research Council, 2013. EP/K026631/1.
[3] Capdesign, Encapsulation of Polymeric Healing Agents in Self-Healing Concrete: Capsule Design, De Belie Nele, 2014.
[4] LORCENIS, LOng Lasting Reinforced Concrete for ENergy Infrastructure under Severe Operating Conditions, European Union's Framework Programme for Research and Innovation Programme under Grant Agreement, 2016, 685445.
[5] –2021 Action CA15202 — Self-Healing as Preventive Repair of COncrete Structures, European Cooperation in Science and Technology (COST). https://www.cost.eu/actions/CA15202/#tabs|Name:overview, 2016. (Accessed 6 October 2023). www.sarcos.eng.cam.ac.uk/.
[6] R.M.4L. Resilient, Materials 4 Life (RM4L), Cardiff University. EPSRC – Engineering and Physical Sciences Research Council, 2017.
[7] EndurCrete, New Environmental Friendly and Durable Concrete, European Union's Framework Programme for Research and Innovation Programme, Grant Agreement, 2018. No 760639.
[8] ReSHEALience, European Union's Framework Programme for Research and Innovation Programme under Grant Agreement No 760824, 2018. www.uhdc.eu.
[9] SMARTINCS, Self-Healing – Multifunctional – Advanced Repair Technologies in Cementitious Systems, European Union's Framework Programme for Research and Innovation Programme under Marie Skłodowska-Curie Grant Agreement SMARTINCS No 860006 Priv. Policy, 2019. Available from: https://smartincs.ugent.be/index. php/about-us.
[10] V. Cappellesso, D. di Summa, P. Pourhaji, N. Prabhu Kannikachalam, K. Dabral, L. Ferrara, M. Cruz Alonso, E. Camacho, E. Gruyaert, N. De Belie, A review of the efficiency of self-healing concrete technologies for durable and sustainable concrete under realistic conditions, Int. Mater. Rev. (2023) 556–603.
[11] C.M. Dry, Repair and prevention of damage due to transverse shrinkage cracks in bridge decks, Smart Struct Mater 3671 (1999) 253–256, https://doi.org/10.1117/12.348675.
[12] R. Davies, O. Teall, M. Pilegis, et al., Large scale application of self-healing concrete: design, construction, and testing, Front Mater 5 (2018) 1–12, https://doi.org/10.3389/fmats.2018.00051.
[13] M.G. Sierra-Beltran, H.M. Jonkers, M. Ortiz, Field application of self-healing concrete with natural fibres as linings for irrigation canals in Ecuador, Fifth International Conference on Self-Healing Materials 32 (2015) 1–4. Durham, NC.
[14] K. Van Tittelboom, J. Wang, M. Araújo, et al., Comparison of different approaches for self-healing concrete in a large-scale lab test, Construct. Build. Mater. 107 (2016) 125–137.
[15] A. Al-Tabbaa, C. Litina, P. Giannaros, et al., First UK field application and performance of microcapsule-based self-healing concrete, Construct. Build. Mater. 208 (2019) 669–685, https://doi.org/10.1016/j.conbuildmat.2019.02.178.
[16] T. Selvarajoo, R.E. Davies, D.R. Gardner, et al., Characterisation of a vascular self-healing cementi-tious material system: flow and curing properties, Construct. Build. Mater. 245 (2020), 118332, https://doi.org/10.1016/j.conbuildmat.2020.118332.
[17] T. Selvarajoo, R. Davies, B. Freeman, et al., Mechanical response of a vascular self-healing cementitious material system under varying loading conditions, Construct. Build. Mater. 254 (2020), 119245, https://doi.org/10.1016/j.conbuildmat.2020.119245.
[18] T. Van Mullem, E. Gruyaert, R. Caspeele, et al., First large scale application with self-healing concrete in Belgium: analysis of the laboratory control tests, Materials 13 (2020) 997, https://doi.org/10.3390/ma13040997.
[19] S. Al-Obaidi, M. Davolio, F. Lo Monte, F. Costanzi, M. Luchini, P. Bamonte, L. Ferrara, Structural validation of geothermal water basins constructed with durability enhanced ultra high-performance fiber reinforced concrete, Case Stud. Constr. Mater. 17 (2022), e01202.
[20] J.R. Tenório Filho, E. Mannekens, K. Van Tittelboom, S. Van Vlierberghe, N. De Belie, D. Snoeck, Innova-tive SuperAbsorbent Polymers (iSAPs) to construct crack-free reinforced concrete walls: an in-field large-scale testing campaign, J. Build. Eng. 102639 (2021) 1–12.
[21] E. Cuenca, V. Postolachi, L. Ferrara, Cellulose nanofibers to improve the mechanical and durability performance of self-healing ultra-high performance concretes exposed to aggressive waters, Construct. Build. Mater. 374 (2023), 130785, https://doi.org/10.1016/j.conbuildmat.2023.130785.
[22] B. Xi, S. Al-Obaidi, L. Ferrara, Effect of different environments on the self-healing performance of ultra high-performance concrete – a systematic literature review, Construct. Build. Mater. 374 (2023), 130946, https://doi.org/10.1016/j.conbuildmat.2023.130946.
[23] M. Davolio, S. Al-Obaidi, Y. Altomare, F. Lo Monte, L. Ferrara, A methodology to assess the evolution of mechanical performance of UHPC as affected by autogenous healing under sustained loadings and aggressive exposure conditions, Cem. Concr. Compos. 139 (2023), 105058, https://doi.org/10.1016/j.cemconcomp.2023.105058.
[24] B. XI, Z. Huang, S. Al-Obaidi, L. Ferrara, Predicting High-Performance Concrete (UHPC) self-healing performance using hybrid models based on metaheuristic optimization techniques, Constr. Build Mater. 381 (2023) 131261, https://doi.org/10.1016/j.conbuildmat.2023.131261.
[25] N.P. Kannikachalam, D. di Summa, R.P. Borg, E. Cuenca, M. Parpanesi, N. De Belie, L. Ferrara, Assessment of Sustainability and self-healing performances of recycled ultra-high-performance concrete, ACI J. 120 (1) 117–132. https://dx.doi.org/10.14359/51737336.
[26] I. Zabalza Bribián, A.V. Capilla, A. Aranda Usón, Life cycle assessment of building materials: comparative analysis of energy and environmental impacts and evaluation of the eco-efficiency improvement potential, Build. Environ. 46 (5) (2011) 1133–1140.
[27] N. Banthia, Fiber reinforced concrete for sustainable and intelligent infrastructure, in: Proc. Of First Int. Conf. on Microstructure Related Durability of Cementitious Composites, Rilem, Nanjing, 2008.
[28] J. R Mackechnie, M.G. Alexander, Using durability to enhance concrete sustainability, Journal of Green Building 4 (3) (2009) 52–60, https://doi.org/10.3992/jgb.4.3.52.
[29] P. Van den Heede, A. Mignon, G. Habert, et al., Cradle-to-gate life cycle assessment of self-healing engin-eered cementitious composite with in-house devel-oped (semi-)synthetic superabsorbent polymers, Cem. Concr. Compos. 94 (2018) 166–180.
[30] P. Van den Heede, N. De Belie, F. Pittau, et al., Life cycle assessment of self-healing engineered cementi-tious composite (SH-ECC) used for the rehabilitation of bridges, in: Life Cycle Analysis and Assessment in Civil Engineering: towards an Integrated Vision Proceedings of the Sixth Inter. Symposium on Life-Cycle Civil Engineering, IALCCE 2018, 2019, pp. 2269–2275.
[31] L. Huang, G. Krigsvoll, F. Johansen, Y. Liu, X. Zhang, Carbon emission of global construction sector, Renew. Sustain. Energy Rev. 81 (2018) 1906–1916.
[32] L. Ferrara, T. Van Mullem, M.C. Alonso, P. Antonaci, R.P. Borg, E. Cuenca, A. Jefferson, P.L. Ng, A. Peled, M. Roig, M. Sanchez, C. Schroefl, P. Serna, D. Snoeck, J.M. Tulliani, N. De Belie, Experimental characterization of the self-healing capacity of cement based materials and its effects on the material performance: a state of the art report by COST Action SARCOS WG2, Construct. Build. Mater. 167 (2018) 115–142.
[33] N. De Belie, E. Gruyaert, A. Al-Tabbaa, P. Antonaci, C. Baera, D. Bajare, A. Darquennes, R. Davies, L. Ferrara, T. Jefferson, C. Litina, B. Miljevic, A. Otlewska, J. Ranogajec, M. Roig-Flores, K. Pain, P. Lukowski, P. Serna, J. M. Tulliani, S. Vucetic, J. Wang, H.M. Jonkers, A review of self-healing concrete for damage management of structures, Adv. Mater. Interfac. 5 (17) (September 2018) 1–28, https://doi.org/10.1002/admi.201800074.
[34] T. Jefferson, E. Javierre, B. Lee Freeman, A. Zaoui, E. Koenders, L. Ferrara, Research progress on numerical models for self-healing cementitious materials, Adv. Mater. Interfac. 5 (17) (September 2018) 1–19, https://doi.org/10.1002/admi.201701378.
[35] S. Al-Obaidi, P. Bamonte, M. Luchini, I. Mazzantini, L. Ferrara, Durability-based design of structures made with UHP/UHDC in extremely aggressive scenarios: application to a geothermal water basin case study, MDPI Infrastructures 5 (11) (November 2020) 1–44, https://doi.org/10.3390/infrastructures5110102.
[36] P. Escoffres, C. Desmettre, J.P. Charron, Effect of crystalline admixtures on the self-healing capability of high performance fiber reinforced concretes in service conditions, Construct. Build. Mater. 173 (2018) 763–774.
[37] D. di Summa, J.R. Tenorio Filho, D. Snoeck, P. Van den Heede, S. Van Vierberghe, L. Ferrara, N. De Belie, Environmental and economic sustainability of crack mitigation in reinforced concrete with SuperAbsorbent Polymers (SAPs), J. Clean. Prod. 58 (July 2022) 1–15, https://doi.org/10.1016/j.jclepro.2022.131998.
[38] M. Maes, K. Van Tittelboom, N. De Belie, The efficiency of self-healing cementitious materials by means of encapsulated polyurethane in chloride containing environments, Construct. Build. Mater. 71 (2014) 528–537.
[39] B. Savija, E. Schlangen, Autogeneous healing and chloride ingress in cracked concrete, Heron 61 (1) (2016) 15–32.
[40] M. Sahmaran, Effect of flexure induced transverse crack and self-healing on chloride diffusivity of reinforced mortar, J. Mater. Sci. 43 (2007) 9131–9136.
[41] S. Jacobsen, E. Sellevold, Self-healing of high strength concrete after deterioration by freeze/thaw, Cement Concr. Res. 26 (1995) 55–62.
[42] M. Ismail, e. al, Effect of crack opening on the local diffusion of chloride in cracked mortar sample, Cement Concr. Res. 38 (2008) 1106–1111.
[43] R. Borg, E. Cuenca, E. GastaldoBrac, L. Ferrara, Crack sealing capacity in chloride-rich environments of mortars containing different cement substitutes and

crystalline admixtures, Journal of Sustainable Cement-Based Materials 7 (3) (2018) 141–159.
[44] E. Cuenca, S. Rigamonti, E. Gastaldo Brac, L. Ferrara, "Improving resistance of cracked concrete to chloride diffusion through "healing stimulating" crystalline admixtures", ASCE Journal of Materials in Civil Engineering 33 (3) (March 2021) https://doi.org/10.1061/(ASCE)MT.1943-5533.0003604. , paper 04020491, pp-1-14.
[45] H. Ling, Q. Chunxiang, Effects of self-healing cracks in bacterial concrete on the transmission of chloride during electromigration, Construct. Build. Mater. 144 (2017) 406–411.
[46] B. Van Belleghem, P. Van den Heede, K. Van Tittelboom, e. al, Quantification of the service life extension and environmental benefit of chloride exposed self-healing concrete, Materials 10 (5) (2017) 1–22.
[47] M. Maes, D. Snoeck, N. De Belie, Chloride penetration in cracked mortar and the influence of autogenous crack healing, Construct. Build. Mater. 115 (2016) 114–124.
[48] E. Cuenca, F. Lo Monte, M. Moro, A. Schiona, L. Ferrara, Effects of autogenous and stimulated self-healing on durability and mechanical performance of UHPFRC: validation of tailored test method through multi-performance healing-induced recovery indices, Sustainability 13 (20) (2021) art. no. 11386.
[49] E. Cuenca, M. Criado, M.C. Alonso, M. Gimenez, L. Ferrara, Durability of ultra-high performance fiber reinforced cementitious composites exposed to chemically aggressive environments: up-grading to ultra-high durability concrete through nano-constituents, ASCE J. Mater. Civ. Eng. 34 (8) (2022), 04022154.
[50] V.C. Li, H.C. Wu, Conditions for pseudo strain-hardening in fiber reinforced brittle matrix composites, Appl. Mech. Rev. 45 (8) (1992) 390–398.
[51] V.C. Li, H. Stang, H. Krenchel, Micromechanics of crack bridging in fibre-reinforced concrete, Mats. & Structs. 26 (8) (1993) 486–494.
[52] V.C. Li, On engineered cementitious composites. A review of the material and its applications, J. Adv. Concr. Technol. 1 (3) (2003) 215–230.
[53] T.N. da Cunha Moreira, V. Krelani, S.R. Ferreira, L. Ferrara, R.D. Toledo Filho, Self-healing of slag cement ultra high performance steel finer reinforced concrete (UHPFRC) containing sisal fibers as healing conveyor, Journal of Building Enginering 54 (August 2022), https://doi.org/10.1016/j.jobe.2022.104638 paper 104638.
[54] F. Lo Monte, L. Ferrara, Tensile behaviour identification in ultra-high performance fibre reinforced cementitious composites: indirect tension tests and back analysis of flexural test results, Mater. Struct. 53 (145) (2020) 1–12.
[55] S. Al Obaidi, P. Bamonte, F. Animato, F. Lo Monte, I. Mazzantini, M. Luchini, S. Scalari, L. Ferrara, Innovative design concept of cooling water tanks/basins in geothermal power plants using ultra-high-performance fiber-reinforced concrete with enhanced durability, Sustainability 13 (17) (2021) art. no. 9826.
[56] J. Qiu, S. He, Q. Wang, H. Su, E.H. Yang, Autogenous healing of fibre/matrix interface and its enhancement, in: G. Pijaudier-Cabot, et al. (Eds.), Proceedings Framcos X, 2019.
[57] F. Lo Monte, L. Ferrara, Self-healing characterization of UHPFRCC with crystalline admixture: experimental assessment via multi-test/multi-parameter approach, Construct. Build. Mater. 33 (May 2021) 1–12, https://doi.org/10.1016/j.conbuildmat.2021.122579, paper 122579.
[58] N. De Belie, K. Van Tittelboom, M. Sánchez Moreno, L. Ferrara and E. Gruyaert, Self-healing concrete research in the European projects SARCOS and SMARTINCS, in Proc. Of the 3rd RILEM Spring Convention and Conference (RSCC 2020).
[59] C. Litina, G. Bumanis, G. Anglani, M. Dudek, R. Maddalena, M. Amenta, S. Papaioannou, G. Pérez, J.L. García Calvo, E. Asensio, R. Beltrán Cobos, F. Tavares Pinto, A. Augonis, R. Davies, A. Guerrero, M. Sánchez Moreno, T. Stryszewska, I. Karatasios, J.M. Tulliani, P. Antonaci, D. Bajare, A. Al-Tabbaa, Evaluation of methodologies for assessing self-healing performance of concrete with mineral expansive agents: an interlaboratory study, Materials 2021 14 (2021) 2024, https://doi.org/10.3390/ma14082024.
[60] M. Roig-Flores, H. Doostkami, M.C. Alonso, L. Ammar, D. Bajare, R. Beltrán Cobos, R.P. Borg, G. Bumanis, A. Darquennes, M. Gimenez, R. Hammoud, M.H. Jonkers, I. Karatasios, A.M. Lozano Násner, S. Papaioannou, M. Reichardt, P. Reiterman, B. Ribeiro, C. Romero Rodriguez, M. Sánchez Moreno, K. Santos, C. Schroefl, P. Serna, Evaluation of the self-healing efficiency of concrete with a crystalline admixture: interlaboratory analysis from COST sarcos RRT3 group, in: Proceedings of 8th International Conference on Self-Healing Materials, ICSHM-MILANO, 2022.
[61] T. Van Mullem, G. Anglani, M. Dudek, H. Vanoutrive, G. Bumanis, C. Litina, A. Kwiecień, A. Al-Tabbaa, D. Bajare, T. Stryszewska, R. Caspeele, K. Van Tittelboom, T. Jean-Marc, E. Gruyaert, P. Antonaci, N. De Belie, Addressing the need for standardization of test methods for self-healing concrete: an inter-laboratory study on concrete with macrocapsules, Sci. Technol. Adv. Mater. 21 (1) (2020) 661–682.
[62] M. Jonkers and C. Romero-Rodriguez, in: RRT6 Concrete with Bacterial Admixtures - SARCOS – Interlaboratory Testing, Delft University of Technology, 2020.
[63] L. Ferrara, V. Krelani, M. Carsana, A fracture testing based approach to assess crack healing of concrete with and without crystalline admixtures, Construct. Build. Mater. 68 (2014) 515–531.
[64] L. Ferrara, V. Krelani, F. Moretti, On the use of crystalline admixtures in cement based construction materials: from porosity reducers to promoters of self-healing, Smart Mater. Struct. 25 (2016), 084002, https://doi.org/10.1088/0964-1726/25/8/084002, 17pp.
[65] E. Cuenca, A. Tejedor, L. Ferrara, A methodology to assess crack sealing effectiveness of crystalline admixtures under repeated cracking-healing cycles, Construct. Build. Mater. 179 619–632.
[66] E. Cuenca, L. D'Ambrosio, D. Lizunov, A. Tretjakov, O. Volobujeva, L. Ferrara, Mechanical properties and self-healing capacity of ultra high performance fibre reinforced concrete with alumina nanofibers: tailoring ultra high durability concrete for aggressive exposure scenarios, Cement Concr. Compos. (April 2021) 17, https://doi.org/10.1016/j.cemconcomp.2021.103956, paper 103956.
[67] A. De Souza Oliverira, O. da Fonseca Martins Gomez, L. Ferrara, E. de Moraes Rego Fairbairn, R.D. Toledo Filho, An overview of a twofold effect of crystalline admixtures: from permeability-reducers to self-healing stimulators, J. Build. Eng. 41 (September 2021) 1–20, https://doi.org/10.1016/j.jobe.2021.102400, paper 102400.
[68] F. Lo Monte, E.J. Mezquida-Alcaraz, J. Navarro-Gregori, P. Serna, L. Ferrara, Experimental Characterization of the Tensile Constitutive Behaviour of Ultra-High Performance Concretes: Effect of Cement and Fibre Type, RILEM Bookseries 36 (2022) 936–946, https://doi.org/10.1007/978-3-030-83719-8_80.
[69] M. Roig-Flores, S. Moscato, P. Serna, L. Ferrara, Self-healing capability of concrete with crystalline admixtures in different environments, Contr. and Build. Mat. 86 (2015) 1–11.
[70] M. Roig Flores, F. Pirritano, P. Serna Ros, L. Ferrara, Effect of crystalline admixtures on the self-healing capability of early-age concrete studied by means of permeability and crack closing tests, Construct. Build. Mater. 114 (July 2016) 447–457.
[71] S. Gupta, S. Al-Obaidi, L. Ferrara, Meta-Analysis and machine learning models to optimize the efficiency of self-healing capacity of cementitious materials, Materials 14 (2021) 1–25, https://doi.org/10.3390/ma14164437, paper 4437.
[72] H. Doostkami, M. Roig-Flores, P. Serna, Self-healing efficiency of ultra high-performance fiber-reinforced concrete through permeability to chlorides, Construct. Build. Mater. 310 (2021), 125168.
[73] L. Ferrara, V. Krelani, M. Carsana, A fracture testing based approach to assess crack healing of concrete with and without crystalline admixtures, Construct. Build. Mater. 68 (2014) 515–531, https://doi.org/10.1016/j.conbuildmat.2014.07.008.
[74] ACI Committee 212, 212.3R-10 Report on Chemical Admixtures for Concrete", American Concrete Institute, 2010, p. 65.
[75] D. Snoeck, N. De Belie, Autogenous healing in strain-hardening cementitious materials with and without superabsorbent polymers: an 8-year study, Front. Mater. 6 (48) (2019) 1–12.